I.O.S.

SUSPENDED PARTICULATE STUDIES OVER THE MADEIRA ABYSSAL PLAIN

BY
W.R. SIMPSON

REPORT NO. 252
1987

OCEAN DISPOSAL OF HIGH LEVEL RADIOACTIVE WASTE
A RESEARCH REPORT PREPARED FOR
THE DEPARTMENT OF THE ENVIRONMENT

NATURAL ENVIRONMENT RESEARCH COUNCIL

INSTITUTE OF
OCEANOGRAPHIC SCIENCES
DEACON LABORATORY

INSTITUTE OF OCEANOGRAPHIC SCIENCES
DEACON LABORATORY

Wormley, Godalming,
Surrey, GU8 5UB, U.K.

Telephone: 0428 79 4141
Telex: 858833 OCEANS G
Telefax: 0428 79 3066

Director: Sir Anthony Laughton, Ph.D., F.R.S.

Natural Environment Research Council

INSTITUTE OF OCEANOGRAPHIC SCIENCES

DEACON LABORATORY

REPORT No. 252

Suspended particulate studies over the Madeira Abyssal Plain

W.R. Simpson

1987

DEPARTMENT OF THE ENVIRONMENT
RADIOACTIVE WASTE MANAGEMENT
RESEARCH PROGRAMME 1979-1987

DoE Report No.: DoE/RW/ 88026

Contract Title: Particulate Matter in the Water Column

Doe Reference: PECD 7/9/214

Report Title: Suspended Particulate Studies Over the Madeira Abyssal Plain

Author: W.R. Simpson

Date of submission to DoE: January 1988

ABSTRACT

Various aspects relating to suspended matter over the Madeira Abyssal Plain are discussed. Special attention is paid to the nepheloid layer including resuspension and transport processes; time variabilities in particle concentrations and fluxes; particle morphology, microbiology and chemical composition; phase association of metals. Also, tentative predictions of the behaviour of some radionuclides are made based on theory and data on rare earth elements. Instrumentation developed for the project is detailed - the deep water particle sampler.

Keywords: 299 DoE sponsored research
155 Aquatic Dispersion
158 Resuspension
225 Ocean sites

This work has been commissioned by the Department of the Environment as part of its radioactive waste management research programme. The results will be used in the formulation of Government policy but, at this stage, they do not necessarily represent Government policy.

CONTENTS

continued .....

CONTENTS continued

BACKGROUND

Outline of report

This report summarises the work conducted over a five-year period at a site on the Madeira Abyssal Plain chosen for a feasibility study into the subseabed disposal of radioactive waste. The programme was structured as follows:

(1) to design, build and prove new instrumentation in order to sample suspended particulates and monitor particle distributions in terms of concentration and size spectra,

(2) to compare this data with other work carried out in the RWD programme,

(3) to characterise suspended particulates morphologically and chemically,

(4) to identify key processes in particle production and fate including particle mass fluxes.

The report is laid out following these main themes.

Relevance of work to RWD

Particles entering the oceans via fluvial and atmospheric transport and biogenic particles produced in situ control the chemistry of the oceans. Uptake of elements from solution may be simplistically viewed as 'active', i.e. biologically mediated, or 'passive', i.e. adsorption on to surfaces and, as such, there can be chemical fractionation between particle types. The ultimate removal of these particles to form sediments, their history in transport, and their subsequent diagenesis is fundamental to deep-sea geochemical cycling of elements. Of relevance to RWD is the characterisation of particulates above the sediment-seawater interface since, in the event of release of radionuclides from sediments, the particle layer above the sediments (the nepheloid layer) becomes a further barrier to, or mechanism for, transport back into the food web.

SECTION 1 - RATIONALE BEHIND AND VALIDATION OF NEW INSTRUMENTATION

RATIONALE BEHIND DEVISED INSTRUMENTATION

Figure 1 shows an idealised particle difference spectrum with the types of particle associated with different size ranges. The main features are that:

(a) As particle size decreases, the particle concentration tends to zero since material effectively becomes dissolved.

(b) The particle maximum in concentration is at about 0.8 μm.

(c) The bulk of the particle concentration is found between 1 and 200 μm.

(d) The tail of the spectrum become asymptotic to the largest size encountered.

Aggregation-disaggregation tends to smooth the distributions, leading to the cumulative number distribution of the type shown in Figure 2. No method available covers the whole size range with one technique thus, in this work, the 1-10 μm range was determined by electron microscopy and the 8-256 μm range by an in-situ particle counter. The cumulative number distribution for this range is given by

$$N_{>8} = a\, d^{-b}$$

and approximates to the straight line

$$\log N = \log a - b \log d$$

In terms of particle counting, the size range chosen was a compromise of flow rate through the sensor head allowing the provision of 'good' statistics for larger particles (256 μm) against the lower cut-off determined by the size that has a small but significant vertical transport

component in terms of settling (8 μm). Particles smaller than this tend to remain in suspension due to Brownian motion. In terms of filter sampling the compromise was for a porosity and diameter of filter that give flow rates of an order to provide sufficient material for analysis. At 1 μm porosity the bulk of material collected is less than 200 μm. Thus, the counting and sampling methods are approximately comparable.

It is the smaller particles that are most important for element removal and concentration, whether biologically produced, e.g. in the surface waters, or whether considering clays versus bacterial adsorption in the nepheloid layer.

The speed of transport to sediments (flux) is primarily an effect of the aggregation of small particles into bigger ones by zooplankton grazing.

DEVELOPMENT AND VALIDATION OF NEW INSTRUMENTATION

The experimental design was discussed in an earlier report (SIMPSON, 1984) and the aims discussed in that report have been met. The instrument built to fulfil those aims, the deep water particle sampler (DWPS), and the validation of the results obtained have also been presented (SIMPSON, GWILLIAM, LAWFORD, LEWIS & FASHAM, 1987). This paper is included as Appendix 1 below. The salient features of the instrument are as follows:

(i) the sensor package includes:

(a) a novel in-situ counter that effectively sizes particles into sixteen ranges between 8 and 256 μm (first cruise 10-174 μm),

(b) a transmissometer which monitors light attenuation proportional to the particle concentration in water, and

(c) temperature and pressure (depth) sensors to give information on water structure.

(ii) a filtration package of four independently operated filters that allows the removal of particles greater than 1 μm using flow rates of about 1 m^3 h^{-1} at midwater depths. The particles so collected can then be subsequently chemically and morphologically analysed.

The operational advantages of such a system are that informed sampling can be carried out on the basis of real-time information from the sensors and the system allows flexibility in that many samples can be taken on one cruise. Disadvantages are that estimates of fluxes are obtained indirectly by modelling of particle data and only for the size range quoted. The information provides a 'snap-shot' of prevailing conditions rather than a time-integrated signal.

Further information will be drawn from Appendix 1 as and when applicable.

SECTION 2 - COMPARISON OF DATA FROM THE DEEP WATER PARTICLE SAMPLER WITH LONG-TERM TRANSMISSOMETER AND SEDIMENT TRAP MOORINGS IN BOTTOM WATERS OVER THE MADEIRA ABYSSAL PLAIN

INTRODUCTION

The validation of the deep water particle sampler as a tool for collecting uncontaminated filter samples and good particle size distribution data for suspended particulate matter was addressed by SIMPSON et al. (1987) Appendix 1. However, the modelling of particle size data went only as far as the calculation of particle volume concentration (Tables 3 & 4 in Appendix 1). Here estimates of particle mass concentration from size distribution are compared to transmissometer and bulk chemical data. Also the estimation of particle mass concentration and particle mass fluxes from size distributions is discussed and compared to estimates of

(a) resuspended mass from long-term transmissometer moorings, and

(b) particle mass fluxes from long-term sediment trap moorings.

INSTRUMENTATION AND STUDY AREA

Table 1 lists cruises, stations worked with the DWPS and CTD-transmissometer and the position and duration of moorings. The study area is shown in Figure 3 and the configuration of the trap and transmissometer moorings are shown in Figures 4 and 5 respectively.

The DWPS is described fully in SIMPSON et al. (1987), Appendix 1. The 1 m pathlength transmissometers were Seatech instruments (BARTZ, ZANAVELD & PAK, 1978) and the mooring details were discussed by SAUNDERS (1987). The sediment traps were built at IOS and have a collection area of 0.575 m^2, are conical funnels of 72° slope, of height 76 cm from mouth to the top of the sample cup. The cup diameter is 5 cm. Chloroform was added to the cups before deployment to prevent microbial degradation of the sample.

TABLE 1 - Log of DWPS Stations and Transmissometer/Sediment Trap Moorings

CRUISE	INSTRUMENT	STATION	MOORINGS	LONGITUDE (°N)	LATITUDE (°W)	DATE	DURATION
RRS Discovery 129	DWPS	10554 #8		31°27.7'	24°25.5'	19.06.82	
RRS Darwin 1/85	CTS/TRANS	8		31°21.0'	24°45.7'	24.02.85	
RRS Discovery 159	DWPS	11287 #1		31°33.5'	24°35.5'	21.05.86	
		#3		31°32.2'	24°34.9'	22.05.86	
		#5		31°33.5'	24°35.5'	22.05.86	
		#6		31°33.6'	24°35.9'	23.05.86	
RRS Darwin 9A/85			Transmissometer	31°33.6'	24°43.4'	20.11.85	182
RRS Discovery 159						21.05.86	
				31°33.6'	24°43.3'	25.05.86	122
RRS Discovery 162						24.09.86	
RRS Darwin 9B/85			Traps	31°32.9'	24°40.2'	10.12.85	172
RRS Discovery 159						21.05.86	
				31°32.9'	24°41.4'	25.05.86	50
RRS Discovery 160						14.07.86	
				31°33.2'	24°40.0'	15.07.86	99
RRS Discovery 163						22.10.86	

SUSPENDED PARTICULATE MASS CONCENTRATION

Transmissometer profiles - were taken on both DWPS and CTD casts. In all cases a clear signal of material resuspended at or transported to the site was observed in the bottom 500 m (Figure 6). The relative changes in percent transmission between the near bottom maximum and midwater minimum were 0.19, 0.20 and 0.15% for June 1982, 1985 and May 1986 respectively. SAUNDERS (1987) calculated that 0.5% light transmission represents 7.5 mg m^{-3} dry weight based on the gravimetric calibrations of BISHOP (1986), thus the above values convert to resuspended concentration maxima over background of 2.9, 3.0 and 2.75 mg m^{-3}, respectively. Integrating from the seabed to 500 m off-bottom the "resuspended" load ranges between 0.56 and 0.75 g m^{-2}.

Particle counter data - can be used to estimate mass based on the assumption that the mass of material between the equivalent sphere diameters d_i and d_{i+1} is given by

$$M_i = n_i \rho_p \pi \bar{d}_i^3/6$$

where n_i is the number concentration of particles between d_i and d_{i+1}, ρ_p is the density of particles of geometric mean diameter $\bar{d}_i$ for that size interval. The values of ρ_p were calculated according to the relationships given in McCAVE (1984). The mass concentration for a given size spectra is the sum of those in the individual channels.

The wet weight mass concentration profile for particles between 10 and 174 μm for Station 10554 is given in Figure 7(a). This profile is based on the data given in SIMPSON et al. (1987), Appendix 1. Table 2 extends the data summary given in Table 4 of SIMPSON et al. (1987) Appendix 1. The resuspended material is about double the concentration of that in the midwater. Also, the change in distribution gradient from - 2.43 to - 2.25 mid- to bottom water, suggests an increase in aggregation in the nepheloid layer. The combined data for the casts carried out on Station 11287 is shown in Figure 7(b), this for particles between 8 and 256 μm. The same general characteristic is observed.

TABLE 2 - Data summary for Station 10554: 10 to 174 μm particles. Values in parentheses are standard errors.

AVERAGE DEPTH z (m)	INTERCEPT log a (no. l^{-1} > 10)	GRADIENT m (no. l^{-1} μm^{-1})	CORRELATION COEFFICIENT r	ATTENUATION c (m^{-1})	PARTICLE MASS CONCENTRATION M (mg m^{-3} wet wt.)	PARTICLE MASS FLUX F (mg m^{-2} d^{-1} wet wt.)
SURFACE (n = 54)						
313	3.703	-2.477	0.997	0.4108	48.5	856.0
(223)	(0.114)	(0.062)		(0.0241)	(5.1)	(142.5)
MIDWATER (n = 171)						
2870	3.033	-2.429	0.997	0.3812	11.6	157.2
(1270)	(0.110)	(0.060)		(0.0014)	(1.0)	(21.1)
DEEP WATER (n = 47)						
5412	3.095	-2.252	0.997	0.3844	17.4	246.8
(48)	(0.104)	(0.056)		(0.0003)	(2.9)	(59.9)

Table 3 summarises data collected whilst filtration was being carried at four heights above bottom. The masses are higher than 10554, probably due to the increase in limits of size range covered.

Also given in Table 3 is the interpolated mass for 0.8 to 8 μm based on the 8 μm best-fit value for the distribution. A cumulative number distribution gradient of - 3 was assumed for this size range (McCAVE, 1975, 1984; SIMPSON et al., 1987). The relative change in mass concentration wet weight from 1000 m ab to 15 m ab was about double that of 10554. From Table 2, the mean in-situ density of the larger aggregated particles is 1.15 g cm^{-3} suggesting a water content of about 90%, thus the dry weight values are estimated to be about 10% of the wet values. For the smaller individual particles of greater density the water content is probably about 70%, thus they account for about 66% of the total mass. The relative increase in dry mass from mid- to deep water is about 3 mg m^{-3}.

Bulk particle chemistry - can provide rough estimates of the total dry weight concentration by scaling up major element concentrations by the stochiometric ratio for the mineral phase with which they are associated. Analysis of filters gave aluminium (or scandium), calcium and iodine values (Table 4) which were scaled accordingly to give estimates of clay, calcite and organic content (Table 5). The combined data from Stations 10554 and 11287 are plotted in Figure 8.

The Ca:Al ratio (Table 4) and calcite:clay (Table 5) show that the coccolithophorid community dominates the surface zone; clay concentrations were low probably due to zooplankton grazing (aggregation into faecal pellets). In deep water the resuspended material is dominated by clays, calcite having been partially dissolved.

Estimated organic concentrations are greatest in surface waters due to production and show a significant increase in the bottom sample compared to midwater due to bacterial production and/or resuspension of organic particles. Clay, calcite and organic concentrations increase by factors of 3, 4 and 5 respectively between 1100 m and 15 m off bottom.

TABLE 3 - Estimates of Mass Concentration from Particle Counter Data: Station 11287

HEIGHT ABOVE BOTTOM (m)	SAMPLE SIZE OF DISTRIBUTIONS IN AVERAGING (number)	1 μm INTERCEPT (log a) (log no. l^{-1})	DISTRIBUTION GRADIENT (b)	WET WT. MASS CONCENTRATION (8-256 μm) ($mg\ m^{-3}$)	0.8 μm† INTERCEPT (log no. l^{-1})	INTERPOLATED WET WEIGHT MASS (0.8-8.0 μm) ($mg\ m^{-3}$)	TOTAL DRY WT.* MASS CONCENTRATION ($mg\ m^{-3}$)
1100	135	5.036	-2.153	13.1	6.092	8.9	3.98
110	325	5.322	-2.209	20.5	6.520	15.4	6.67
25	162	5.295	-2.179	22.1	6.327	15.4	6.83
15	153	5.293	-2.162	23.8	6.341	15.8	7.12

† Calculated as follows: At 8 μm, $\log N_{>8} = \log a - b \log 8$

$$\log a_{0.8} = \log N_{>8} + 3 \text{ (for small particle gradient } b = 3)$$

$$M_{0.8}^{8.0} = - \pi\ a_{0.8}\ \ln(8/0.8)\ \rho_p/2 \times 10^6 \text{ (for } \rho_p = 2)$$

* Assumed water content for 8-256 μm of 90%, 0.8-8.0 μm 70%

TABLE 4 - Scandium, aluminium, calcium and iodine particulate concentration from GME (ng l^{-1}). Depth, z, in meters.

	z	Sc	Al	Ca	I	Ca/Al
	120	-	50	3940	18.2	78.8
	134	0.0034	27*	1242	-	46.0
	750	-	28	1100	1.6	39.3
	1320	0.0105	84*	812	-	9.7
	1806	0.0105	84*	503	-	6.0
	2300	-	90	630	4.3	7.0
+	1000	-	66	160	0.2	2.4
+	100	-	190	200	0.1	1.1
+	25	-	266	460	0.7	1.7
+	15	-	279	440	1.0	1.6
+	5	0.0295	236*	475	-	2.0

* [Al] = [Sc] x 8 x 10^3 (Cruise 129 only).

+ Depth off-bottom

TABLE 5 - Estimates of the Concentration of Major Components of the Suspended Particulate Matter: Station 11287

($ng\ l^{-1}$)

DEPTH (m)	CLAY	CALCITE	ORGANICS	OPAL	TOTAL ($mg\ m^{-3}$)	$\frac{CALCITE}{CLAY}$
120	250	9850	19,950	3339	33.4	39.4
750	135	2750	1,753	515	5.2	20.3
2300	450	1575	4,714	749	7.5	3.5
+ 1100	330	400	219	105	1.1	1.2
+ 110	950	500	110	173	1.7	0.5
+ 25	1330	1150	767	360	3.6	0.9
+ 15	1395	1100	1,096	399	4.0	0.8

where [CLAY] = [Al] x 5

[CALCITE] = [Ca] x 2.5

[ORGANICS] = [I] x 945 x 1.16, i.e. [I] x (C:I) x Redfield Ratio

[OPAL] = 10% TOTAL

\+ Depth off-bottom

These observations are supported by scanning electron microscope analysis of samples (Figure 9 in SIMPSON et al., 1987; Appendix 1). There is an excess of 3 mg m^{-3} between the midwater minimum and the near-bottom sample from the combined estimate of mineral phases (Table 5).

Long-term variation in suspended particle concentration - was reported by SAUNDERS (1987) (Fig. 7). The break in the record occurred whilst the mooring was being serviced and the transmissometers exchanged. This was carried out during the occupation of Station 11287. From this record it can be seen that the station was worked over a period of low particle loading and weak current activity (Fig. 7). At no time in the 304 days did the suspended load exceed 5 mg m^{-3} over the background concentration. Highest concentrations were seen between January and March 1986. This mooring will be discussed further in relation to the trap data.

Comparison of methods - the data on particle mass concentrations is summarised in Table 6. Bearing in mind the disparity of the methods involved the agreement is good. The differences from minimum to maximum values for each method range from 2.9 to 3.9 mg m^{-3} the same as the SAUNDERS (1987) estimate. There is fairly good overall agreement between particle counter models and transmissometer data yet the total chemical estimates are a factor of 2 to 4 lower.

PARTICLE MASS FLUXES

Particle counter data - can be modelled to estimate the rate of mass movement of material through the oceans (McCAVE, 1975). The settling velocities of a population of particles of mean diameter $\bar{d}_i$ is assumed to follow Stokes' Law:

$$\bar{U}_i = \frac{g\Delta\rho\ \bar{d}_i^2}{18\ \eta} \qquad (m\ d^{-1})$$

where g is gravity, $\Delta\rho$ is the density difference between the particle and seawater, and η is the viscosity of the seawater. The density and viscosity of seawater were determined from CTD measurements and particle density and mean diameter calculated as indicated above. Thus, for each

TABLE 6 - Data Summary of Mass Concentration Estimates: Station 11287
(mg dry wt. m^{-3})

HEIGHT ABOVE BOTTOM	TRANSMISSOMETER v. GRAVIMETRIC	PARTICLE COUNTER (MODELLED) 8-256 μm	INTERPOLATED PARTICLE DATA 0.8-256 μm	CHEMICAL ANALYSIS (MAJORS)
1100	4.0	1.31	3.98	1.1
110	5.95	2.05	6.67	1.7
25	6.1	2.21	6.83	3.6
15	6.25	2.38	7.12	4.0
Δ MAX/MIN	2.25	1.07	3.14	2.9

size interval (channel) of the particle counter the total mass flux is given by

$$F = \Sigma M_i \cdot U_i \qquad (mg\ m^{-2}\ d^{-1})$$

Included in Table 2 for Station 10554 (10-174 μm) was the estimated fluxes in surface, mid- and bottom waters. Most of the material in surface waters is intensively recycled by the biota; little escapes to depth. The mean midwater flux is 157 mg m^{-2} d^{-1} wet weight compared to a deep water flux of 247 mg m^{-2} d^{-1}. The more detailed Station 11287 (8-256 μm) gave wet weight fluxes of 244, 359, 379 and 471 mg m^{-2} d^{-1} at 1100, 110, 25 and 15 m above bottom during filtration runs (Table 7). The greater fluxes are due in part to the wider size range under consideration. Note that the mean settling velocity is between 17 and 20 m d^{-1} for this population of particles compared to 14 m d^{-1} for 10554. It is not necessary to consider particles < 8 μm since their contribution to the total flux is small but the estimate of 90% water content holds and the fluxes need to be divided by 10 in order to estimate the dry weight flux. These estimates can be compared directly to sediment trap data.

Sediment trap fluxes - are calculated simply by measuring the dry mass of material collected, M, and dividing by the product of the collection area, a, and the duration of the deployment, t:

$$F = \frac{M}{a\ t} \qquad (mg\ m^{-2}\ d^{-1})$$

The duration of deployments A, B and C were 172, 50 and 99 days respectively. Table 7 and Figure 10 show the measured fluxes at given heights above the seabed.

Deployment A covered the period December 1985 to May 1986,the trap at + 3 m giving the maximum in measured flux of 54.3 mg m^{-2} d^{-1} and at + 10 m, 46.4 m^{-2} d^{-1}. For the deployments B and C combined (May to October), the + 10 m average flux of 28.9 mg m^{-2} d^{-1} was about half of the previous six months. Essentially the order of decreasing flux is Winter - Spring > Late Summer - Autumn > Summer.

TABLE 7 - Particle Mass Fluxes at GME (mg. dry wt. m^{-2} d^{-1})

HEIGHT ABOVE BOTTOM	STATION 10554 (10-174 μm)	STATION 11287 (8-256 μm)	SEDIMENT TRAPS			
			LARGE PARTICLE FLUXES			
(m)	June 1982	May 1986	Dec. 1985 May 1986	May to July 1986	July to Oct. 1985	Dec. 1985 Oct. 1986
'1000'	15.7	24.4	43.1	15.6	25.1	33.3
'100'	24.7	35.9	34.3	12.6	16.1	25.3
25		37.9				
15		47.1				
10			46.6	25.0	30.8	38.4
3			54.3			

The 321 day averaged supply of material at + 1000 to + 1200 m is 33.3 mg m^{-2} d^{-1}, at + 100 to + 120 m is 25.3 mg m^{-2} d^{-1} and at + 10 m, 38.4 mg m^{-2} d^{-1}. The observed decrease in flux at '100 m' compared to '1000 m' may be due to disaggregation followed by dissolution. The seasonal variation in percent organic carbon content was small, although slightly greater values were evident during the winter-spring period (4.4%:3.7%).

Comparison of methods - Both methods, modelled particle-counter data versus direct measurement, have limitations. There is the $\bar{d}_i^5$ dependence in modelled fluxes which will be a source of error, yet traps are poorly understood in terms of collecting efficiencies, particularly for small particles. The size range of particles being sampled will overlap and the differences that emerge can be used to advantage.

The first point to note is that the overall agreement is good; within a factor of 2 or better.

Second, particle counter data, supported by transmissometer data, show an increased particle concentration from + 1000 to the bottom, whereas the low observed at 100 m with traps appears anomalous. However, the apparent 'loss' of material of about 20 to 25% between these traps could account for part of the 'gain' (32%) in material seen by the particle counter. The distribution gradient at 110 m (Table 3) becomes more negative and the intercept values increase supporting the idea of disaggregation between 1000 m and 100 m off-bottom.

Third, part of the increased flux in the winter-spring deployment could be due to resuspension as seen in the transmissometer mooring (Fig. 7), although increased production in surface waters during the spring bloom seems to have a greater affect on particle supply to deep waters.

Lastly, the difference in organic C (20% on filters, 4% in traps) probably reflects the amount of bacterial production (see Section 3).

DISCUSSION

Resuspension or Transport?

Consider three types of individual particle representative of GME sediments, clays, coccoliths of E. huxleyi and bacteria. Their mean diameters and densities are 1.6 (LAMBERT et al., 1981) 2.4 and 0.8 μm (PATCHING, pers. comm.) and 2.2, 1.4 and 1.1 g cm^{-3} respectively.

The critical friction velocity to initiate motion of particles, U_* can be derived from the relationship

$$\frac{\rho\, U_*^2}{\Delta\rho\, g\, \bar{d}} \approx 0.1 \left[\frac{U_* n \bar{d}}{\rho}\right]^{-0.3}$$

where ρ is the density of seawater (all other parameters as given above).

The resulting values for U_* for clay, calcite and bacteria are 0.33, 0.14 and 0.06 cm s^{-1}. SAUNDERS (1987) also gave the relationship for the friction velocity at the sediment-seawater interface and the mean flow at some height off the bottom to be dependent on the drag coefficient, C_D, thus:

$$U_{10m} = U^* C_D^{-\frac{1}{2}}$$

For GME it was calculated that $C_D^{-\frac{1}{2}} = 34$ therefore the + 10 m current velocities required to move clay, calcite and bacteria are 11.2, 11.6 and 2 cm s^{-1}. Furthermore, WEAVER, BUCKLEY and KUIJPERS (in press) found that the mean grain size of surface sediments at the Madeira Abyssal Plain was 2 μm thus assuming non-cohesion, a + 10 m current of 11 cm s^{-1} will be required to initiate movement. Current meter measurements on the plain at + 10 m showed that currents only exceeded 10 cm s^{-1} for 71 hrs in 23,000 hrs, i.e. for 27 hours per annum, therefore erosion at GME is probably a rare event and only very fine (< 1 μm) material is constantly reworked. That small organic particles move more easily helps to explain the higher organic content of filter samples compared to trap material.

The mean size of 2 μm also suggests that large aggregates are rapidly broken down (BILLETT et al., 1983).

The settling time of fine particles under Stokesian settling is long (e.g. for 100 m: 880 years at 0.1 μm, 10 years at 1.0 μm, 1 year at 4 μm, and 85 days at 10 μm) and the Brownian aggregation of small particles can be shown to be insignificant at the concentrations encountered at GME as follows. McCAVE (1984) demonstrated that the particles that undergo Brownian diffusion (< 8 μm) have a probability of colliding given by the coagulation kernel, K,

$$K = \frac{2\,k\,T}{3\,\eta}\,\frac{d_{ij}^{\,2}}{d_i\,d_j}$$

and that the time taken to reduce the original concentration, N_o (number l^{-1}), of a monodisperse suspension by half is

$$t_{\frac{1}{2}} = 3\eta/kTN_oE$$

where k is Boltzmann's constant (1.381×10^{-16} g cm^2 s^{-2} K^{-1}), T is absolute temperature (275°K), η is viscosity (0.016 g cm^{-1} s^{-1}), dd_{ij} is the sum of the particle diameters of size d_i and d_j and E is the efficiency of collision-coagulation. For example, a range of concentrations of 1×10^3 to 1×10^4 particles cm^{-3} at 0.8 μm, typical of GME, give

$$t_{\frac{1}{2}} = 3.16 \times 10^{12}/N_oE \text{ (sec) or } 1 \times 10^5/N_oE \text{ (yr)}$$

or $t_{\frac{1}{2}}$ between 10 to 100 years at 10% efficiency or 1 to 10 year at 100% efficiency.

Thus it seems likely that the fine particles in the nepheloid layer have been transported over great distances to the site and will remain in suspension until particle concentrations are sufficiently great for Brownian coagulations to be significant. However, this does not take into account the effect of biological ingestion and excretion as an accelerator of the aggregation process.

Mass Fluxes and Sediment Accumulation Rates

The mass fluxes measured are consistent with other measurements made over abyssal plains in low production areas of the Western Atlantic, i.e. Sohm Abyssal Plain - April 1978 to August 1986 - at + 1000 m in 4200 m, 15.6 to 85 mg m^{-2} d^{-1} (DEUSER, ROSS & ANDERSON, 1981; JICKELLS, DEUSER & KNAP, 1984) and at various depths in 5581 m, 13-69.4 mg m^{-2} d^{-1} (HONJO, 1978, 1980); Demerara Abyssal Plain at various depths in 5288 m, 47-69 mg m^{-2} d^{-1} (HONJO, 1980). However, the primary flux at the site ($\geq$ 25 mg m^{-2} d^{-1}) outweighs the sediment accumulation rate. This rate was determined to be 0.5 cm/10^3 yr which, based on the known water content of 50% and dry weight density of 2.2 g cm^{-3}, is equivalent to a dry weight flux of 15 mg m^{-2} d^{-1}, or 5.5. g m^{-2} yr^{-1} (COLLEY, pers. comm.). Obviously the comparison of long-term (100 yr) with short-term (1 yr) fluxes does not allow for the possibility of small-scale fluctuations but dissolution of calcite and uptake by biota and/or remineralisation of organics could account for some of the difference. Also remobilisation due to the 'rare' high current event (SAUNDERS, 1987) could move some of the material from the site but at present the nepheloid layer contains only 0.56-0.75 g m^{-2} or the equivalent of 10% to 14% of the annual accumulation.

CONCLUSIONS

1. There is good agreement between calibrated transmissometer and modelled particle counter data.

2. From light transmission, size spectra and chemical methods the nepheloid layer concentration is 3 mg m^{-3} above the midwater minimum values.

3. The long-term concentration in the nepheloid layer does not exceed 5 mg m^{-3}, i.e. the nepheloid layer at GME is weak.

4. Resuspension at the site will occur rarely and only effect particles < 1 μm. Organics are likely to be preferentially moved.

5. The nepheloid layer is probably transported to the site from local topographic highs and/or the ocean margins.

6. Brownian aggregation is likely to play a minor role in sedimentation.

7. Disaggregation of large particles between 1000 m and 100 m occurs.

8. There is good agreement between trap and modelled particle counter fluxes and sediment accumulation rates (15 to 25 mg m^{-2} d^{-1}).

9. The implication is that, should radionuclides escape from the seabed or be introduced at the sediment-seawater interface and subsequently adsorbed on to particles, they will be transported great distances or until the nepheloid layer particle concentration is great enough for Brownian coagulation to be a significant removal process. This will be addressed in the following section.

SECTION 3 - MICROBIOLOGY, ELEMENT ENRICHMENTS IN PARTICLES AND PARTICLE SURFACE CHARGE OVER THE MADEIRA ABYSSAL PLAIN

INTRODUCTION

In this section the aim is to tie together the chemical, biological and physical aspects of element scavenging and attempt to predict how radionuclides will behave in sea water should they be released at the sediment-seawater interface.

METHODOLOGY AND SAMPLING

Results discussed in this section were obtained from RRS Discovery Cruises 125 (THOMSON, 1982), 129 (WILSON, 1982), 147 (SIMPSON, 1984), 148 (ROE, 1984) and 159 (SIMPSON, 1987) - all in the NE Atlantic. Station positions will be given in the text or figures. Bacterial and phytoplankton samples were taken by CTD-rosette casts and suspended particulates for surface charge and elemental analysis by large volume filtration through 1 μm Nuclepore membranes using the deep water particle sampler (SIMPSON et al., 1987; Appendix 1).

Bacteria were counted by epifluorescence microscope analysis. Water samples (20 ml) were taken from water bottles and fixed with 40% formalin (2 ml) and stored at 4°C. Acridine orange (0.2 ml of 1 g l^{-1}) was used as the stain.

For phytoplankton analysis, water samples of about one litre were filtered through 0.4 μm Nuclepore membranes. Membranes were rinsed with distilled water to remove excess salt, air dried and subsequently analysed by scanning electron microscopy.

Subsamples of sea water were also taken and transferred to growth media then incubated in light at 15°C for later examination.

Nuclepore (1 μm) membranes (29.3 cm diameter), used on the DWPS to collect suspended particulates, were rinsed with distilled water, air dried and later analysed by instrumental neutron activation analysis (SIMPSON et al., 1987; Appendix 1).

Preparations for surface charge analysis were made by resuspending particles from 4 cm^2 section membranes cut from DWPS samples. Analysis was carried out by electrophoretic mobility determinations using filtered deep ocean water as media.

MORPHOLOGY

Scanning electron microscopy with energy dispersive X-ray analysis was used to characterise particles from GME and other stations in the subtropical NE Atlantic. Figure 11 shows results for 1-10 μm particles in the GME region (left and middle column). Calcium, in the form of coccolith calcite, dominates all depths but the alumino-silicate fraction (clays) significantly increases with depth to give a high proportion of the total in the nepheloid layer. Of the minor components, the organic and opal ratios decrease with depth allowing sand (quartz) grains to be more readily identified in deep samples.

For the 10 to 100 μm particles (Figure 12) calcium in the form of coccospheres and coccoliths aggregated in faecal material dominate. Identifiable clay aggregates are limited to about 20 μm maximum and identifiable diatom and radiolarian tests (opal) peak between 20 and 40 μm. Amorphous organic aggregates are in relatively high abundance from surface to mid-waters. Thus from this simple analysis, irrespective of size, coccolithophorid calcite dominates the 1 μm to 100 μm fractions. Alumino-silicates are significant from 0.2 μm (LAMBERT, JEHANNO, SILVERBERG, BRUN-COTTAN & CHESSELET, 1981) to about 20 μm and are particularly evident in deep water. There also appears to be a dramatic decrease in the organic component from surface to depth.

MICROBIOLOGY

The bulk of the particle assemblage is derived from the phytoplankton and thus it was decided to look in more detail at the community structures of the micro-organisms at GME. These organisms are involved in primary fixation of material and, therefore, the active uptake of elements from solution. Bacteria may also be primary producers yet also degrade and recycle detritus.

Bacteria - Bacterial samples were collected on Cruises 147 and 159. To date, the stations along 42°N have been worked up: 11097 (10°W) to 11101 (25°W) (PATCHING, pers. comm.). Bacteria were nearly always free, i.e. not attached to particle surfaces; there were a few instances when clumps were observed but only in surface waters. The frequency of dividing cells (% FDC) was also noted and population doubling times were calculated to be 8.8 to 28 hr, based on the expression

$$P.d.t. = 0.693/\mu$$

where μ (the instantaneous growth rate constant, h^{-1}) =

$$0.299\ FDC - 4.961$$

The concentrations ranged from 2 to 6 x 10^8 l^{-1}, from surface to 100 m; 1 to 3 x 10^8 l^{-1}, from 100 m to 2000 m; 0.6 to 1 x 10^8 l^{-1}, from 2000 m to within 100 m of the bottom; and 1 to 3 x 10^8 l^{-1}, in bottom waters. The concentrations at GME are likely to be lower than this due to the lower surface production in the subtropics, but probably not by more than a factor of two.

Phytoplankton community structures - Coccolithophorids are phytoplankton that lay down calcareous tests. Generally, the phytoplankton community of the sub-tropical region of the NE Atlantic is dominated by coccolithophorids (Fig. 13), irrespective of time of sampling (pers. comm. R. JORDAN). There are, however, changes in family and species dominance during the annual cycles. This can clearly be seen in Figures 14 and 15. In near-surface waters the holococcoliths, those made of individual microcrystals, dominate, yet due to their fragility and rapid dissolution

are rarely seen at depth. Of the more robust forms, the heterococcoliths, E. huxleyi dominates as it does in most of the world's oceans. It gives way to U. tenuis in the summer months. One interesting observation is that as the water depth increases, the degree of complexity of coccolith structure and calcification increases. Why this happens is unknown but it may influence the distributions of elements laid down with the calcium in calcite as, for example, Cd and possibly the rare earth elements.

Protozoans - As a group, very little is known of microprotozoans in seawater. In attempting to isolate coccolithophorids sampled at sea into pure culture in the laboratory, problems were encountered due to the presence of protozoans at high concentration and in the size range 1 μm to 100 μm (R. JORDAN, pers. comm.). Zooplankton grazing is yet to be assessed.

CHEMISTRY OF TRACE METALS

Although the gross change of particle type with size and depth can be appreciated it tells us little of the absolute change in concentrations of the elements from which the particles are made. Major elements (Al, Ca, Si, I) are discussed in Section 2. For the trace metals it is best to look at their enrichments in particulates against their background concentration in the continentally derived clay component. It is assumed that Sc or Al concentrations are derived only from clays and hence can be taken as unity. Since the concentrations of the other elements in continental clays are known, their relative enrichments in particulates from in-situ processes can be derived. Table 8 and Table 9 show results for some elements from Cruise 129 and Cruise 159 respectively. As can be seen, Th, Fe and Mn give EF values close to the shale concentrations whereas Co, Ba and V show some enrichment particularly in surface and near-surface waters, probably due to involvement in biological metabolism. The remainder of the elements (Sb, Ag, Se, Hg and Au) are known as the volatile elements with enrichments partly due to fallout of atmospheric particles containing high concentration of these elements and partly through active concentration by the biochemical pathways of the organisms living in surface and near-surface waters. This effect is clearly seen in Figure 16 where the top 2500 m values and the deep

TABLE 3

(a) **Particulate Element Concentration**
($ng\ l^{-1}$), 1-60 μm particles

	134 m	1320 m	1806 m	5470 m
Sc	0.0034	0.0105	0.0105	0.0295
Th	0.0038	0.0116	0.0118	0.028
Fe	13.45	36.38	54.22	87.3
Co	0.0307	0.0505	0.0799	0.0759
Sb	0.0279	0.0528	0.0834	0.0245
Ag	0.0103	0.2537?	0.0350	0.0134
Se	0.0711	0.0516	0.0507	0.0279
Hg	0.1040	0.0513	0.1307	0.0721

(b) **Crustal Enrichment Factors:**

$$E.F._C = ([Element]/[Sc])_{particles}/([Element]/[Sc])_{crust}$$

	134 m	1320 m	1806 m	5470 m	$([El]/[Sc])_{crust}$
Th	2.6	2.5	2.7	2.2	0.436
Fe	1.5	1.4	2.0	1.2	2559
Co	7.9	4.2	6.7	2.3	1.136
Sb	903	553	873	91	9.091×10^{-3}
Ag	953	-	1048	143	3.182×10^{-3}
Se	9212	2167	2130	417	2.272×10^{-3}
Hg	8400	1342	3419	671	3.636×10^{-3}

TABLE 9

(a) **Particulate Element Concentration**

($ng\ l^{-1}$)

	120 m	750 m	2300 m	+ 1000 m	+ 100 m	+ 25 m	+ 15 m
Al	50	28	90	66	190	266	279
Mn	3.5	11.5	16.9	2.4	5.2	7.6	8.8
V	1.67	0.29	0.06	0.2	0.8	0.13	0.21
Ba	20.3	14.4	26.3	16.3	4.8	10.0	11.5

(b) **Crustal Enrichment Factors:**

$$E.F._c = ([Element]/[Al])_{particles}/([Element]/[Al])_{crust}$$

	120 m	750 m	2300 m	+ 1000 m	+ 100 m	+ 25 m	+ 15 m	$([El]/[Sc])_{crust}$
Mn	6.1	35.7	16.3	3.2	2.4	2.5	2.7	1.15×10^{-2}
V	11.8	13.0	0.8	3.8	5.2	6.2	1.0	8×10^{-4}
Ba	78.1	98.9	56.2	4.75	4.9	7.2	7.9	5.2×10^{-3}

TABLE 10. Rare Earth Element Concentrations (mol kg^{-1} $x10^{12}$), Distribution Coefficients (K_D) and Shale Enrichment Factors (vs. Sc)

e-S Region		Surface	Near Surface	"Mediterranean"	Deep Water	Bottom Water		
Sample)Water Depths) (m))Particles		0 28	100 & 200 134	1000 & 1500 1320	2500 & 3000 1806	4500 5470	Shale Concentration ($nmol.\ g^{-1}$) a) Ref 9	b) Ref 10
La - dissolved		36.7	15.0	22.8	31.0	54.4		
particulate		n.d.	0.0897	0.549	0.492	0.581		
K_D		-	$1.8x10^5$	$5.0x10^6$	$3.3x10^6$	$1.1x10^6$		
E.F. Shale	a)	-	1.4	2.8	2.5	1.1	213	
	b)	-	1.2	2.4	2.1	0.91		295
Ce - dissolved		65.3	19.6	15.3	22.7	55.1		
particulate		0.500	0.421	1.501	1.549	2.213		
K_D		$8.8x10^4$	$6.3x10^5$	$2.0x10^7$	$1.2x10^7$	$4.2x10^6$		
E.F. Shale	a)	3.5	3.3	3.8	3.9	2.0	428	
	b)	3.0	2.6	3.2	3.4	1.7		592
Eu - dissolved		0.615	0.747	0.982	0.941	1.22		
particulate		0.0077	0.0071	0.0102	0.0095	0.0213		
K_D		$9.1x10^4$	$2.8x10^5$	$2.2x10^6$	$2.0x10^6$	$1.8x10^6$		
E.F. Shale	a)	3.0	3.1	1.5	1.4	1.1	7.63	
	b)	2.6	2.6	1.2	1.2	0.94		10.5
Yb - dissolved		3.15	3.81	4.99	5.00	5.16		
particulate		0.0253	0.0158	0.0179	0.0184	0.0302		
K_D		$1.4x10^5$	$1.2x10^5$	$7.4x10^5$	$7.6x10^5$	$6.2x10^5$		
E.F. Shale	a)	6.9	4.8	1.8	1.8	1.1	10.9	
	b)	4.4	3.1	1.1	1.2	0.7		20
Sc - particulate		0.0824	0.0736	0.226	0.225	0.624	245	289

Dissolved concentration - from ref. 1; In the equations described square brackets denote concentrations; $K_D = \rho.f/(1-f)[m]$ where f = [REE] particles/$[REE]_{total}$ and [m] = particle mass concentration; $E.F._{shale} = ([REE]/[Sc])_{particles}/([REE]/[Sc])_{sha}$

Ref 9 = Cody Shale values Ref. 10 = Wedepohl shale values.

water values have been averaged. The enrichments in deep waters are lower for two main reasons. First, the nepheloid particles are rich in clays relative to biogenic components and hence the samples are "diluted". Secondly, the organic and calcite contents are much lower than in surface waters hence the authigenic enrichment is lower.

The rare earth elements La, Ce, Eu and Yb have been considered separately (Table 10). The enrichments are low, between 1 and 7, yet the estimated K_Ds, using ELDERFIELD AND GREAVES' (1982) solution data, show that the system is non-steady state. Cerium is known to exist as Ce IV and to be more reactive than the + III oxidation state possessed by the rest of the REE. This is reflected by the consistently high enrichment factor. Also of interest is that there is an increase in concentration towards the bottom in both dissolved and particulate phases.

Particle surface charge - The electrophoretic mobilities of small particles from GME cruises were measured by LODER AND LISS (1982) and P. NEWTON (pers. comm). In every case the particles were found to carry a negative surface charge due to the adsorption of organics to particle surfaces (Fig. 17).

DISCUSSION

Element Scavenging and Transport

The problem with element scavenging, a loose term that covers a multitude of processes but is generally applied to clay particles, was succinctly summarised by BREWER AND HAO (1979) in that the number of free hydroxyl groups on clay particles required to remove elements from sea water would outweigh the particulate matter in sea water by 1.3×10^2. They concluded that "the concept of horizontal diffusion towards a boundary and adsorption at the sediment-water interface may have much merit". But then how does this mechanism work? A further problem with scavenging is that many of the elements have negatively-charged complexes in solution (WHITFIELD & TURNER, 1981) and particulates are all negatively charged (LODER & LISS, 1982; P. NEWTON, pers. comm.). Exchange mechanisms

TABLE 11 - Relative Surface Area Concentrations of Clays, Calcite Particles (Emiliana huxleyi coccoliths) and Bacteria in Sea Water.

		CLAYS	CALCITE	BACTERIA	
Mean diameter (μm)		1.6	2.2	0.8	
Equivalent sphere surface area x 2 (μm^2)		16	32*	4	
Particle density (g cm^{-3})		2.2	1.4*	1.1	
Particle mass (μg)		9×10^{-6}	8×10^{-6}*	3×10^{-7}	
Mass concentration** ($\mu g\ l^{-1}$)	NEAR SURFACE	0.25	9.9	3.0***	
	MIDWATER	0.33	0.4	1.8***	
	DEEP	1.4	1.1	3.0***	
Number concentrations of particles (no. l^{-1})	NEAR SURFACE	2.8×10^{4}†	1.2×10^{6}†	1×10^{8}	(1-3)
	MIDWATER	3.7×10^{4}†	5.0×10^{4}†	0.6×10^{8}	(0.6-1)
	DEEP	1.6×10^{5}†	1.4×10^{5}†	1×10^{8}	(1-3)
Surface area concentration†† ($\mu m^2\ l^{-1}$)	NEAR SURFACE	4.5×10^{5}	2.6×10^{7}	4×10^{8}	
	MIDWATER	5.9×10^{5}	$1,6 \times 10^{6}$	2.4×10^{8}	
	DEEP	2.6×10^{6}	4.5×10^{6}	4×10^{8}	

* Honjo (1977).

** Taken from Section 2.

*** Individual mass (3×10^{-7}) x no. concentration/10, i.e. 90% water assumed.

† Mass concentration/Particle mass.

†† Number concentration of particles x surface area.

proposed by SCHINDLER AND STUMM (1987) have similar problems to those mentioned above, i.e. insufficient OH groups to allow for exchange.

However, the work in the deep NE Atlantic has shown that free-floating bacterial surfaces could be 100 times greater than the sum of clay and calcite (Table 11). In this table are presented the physical data for particles. The mass given for an individual bacterium is the wet weight which has been converted to a dry weight for direct comparison with clays and calcite (mass taken from Section 2). The other calculations are straightforward: i.e. no. concentration = mass concentration/particle mass (bacteria were measured directly) and total surface area = no. concentration x (equivalent sphere surface area x 2). The factor of 2 was measured directly on coccoliths (HONJO, 1977), assumed for clays on the basis of interstitial surfaces and assumed for bacteria because of the outer membrane present in marine bacteria. Hence it is derived that marine bacteria could offer as much as 100x the surface area of other small particles.

This has far-reaching consequences in that

(a) elements not only can be passively adsorbed to the surfaces but also the negative solution complexes may encounter acid pH at the cell membrane and hence be actively absorbed as positive complexes,

(b) bacteria have sufficient low density and small size to be moved from the sediment surface by low bottom currents monitored at 31°N over the Madeira Abyssal Plain (clays and calcite are thought to be immobile).

Recall that resuspension at this site was thought to be minimal and thus the weak nepheloid layer was transported across the site from some distance away and Brownian aggregation (Section 2) was shown to be insignificant at this site. Thus remineralised material readsorbed on to bacterial (or in solution) may be transported over great distances to the margin where conditions may favour removal (e.g. high particle loads or biological scavenging). The role of the protozoan/bacterial loop in this process is yet to be assessed.

Prediction of behaviour of the radionuclides - The nearest we can come to predicting the behaviour of the transuranics in sea water is to compare some of the properties of these elements, e.g. charge, and ion diameter, with other heavy elements of variable oxidation state, e.g. REE. This discussion is tentative but may give some indicators.

First, consider the table of oxidation states of the elements in Figure 18 divided into the isoelectronic structures of the outer electron shell (right-hand column). It is assumed that Am, Cf and Ac have oxidation states of + 3, cf. REE; Pu + 4, cf. Ce and Th; and Np + 5, cf. Ta, Pa. Second, if the energy coefficients for these oxidation states are calculated (ROESLER & LANGE, 1972), some interesting patterns emerge (Fig. 19):

(a) The element order is primarily controlled by the isoelectronic structure.

(b) This orders the elements in the sequence of mineral character (see WHITFIELD & TURNER, 1979), and

(c) biological character.

(d) The horizontal line denotes the speciation in sea water (WHITFIELD & TURNER, 1981).

Thus, Ac III bears a close resemblance to La III; Np V and Pu IV fall in the same zone as Ce IV, Th IV, Pa V and Ta V; and Am III occurs with the light rare earth III series.

The simplest analogy, then, is for those in the Ce/Th group to form hydroxides in sea water and those behaving like the lanthanides to form mono- and di-carbonate complexes with a small percentage (< 10%) present as free ions (CANTRELL & BYRNE, 1987). Residence time estimates (t) of the rare earths in deep water were calculated using the relationship given in BACON AND ANDERSON (1982) from the data supplied in Table 10. For La, Ce, Eu and Yb, respectively, the ranges of t are 255-510 yr, 65-130 yr, 505-1010 yr and 1395-2770 yr, respectively. These fall in the ranges quoted in ELDERFIELD AND GREAVES (1982). Also Th has a deep-ocean

residence time of 40 yr. Residence times of the order of 100 yrs can be expected for Pu, about 200 to 500 yr for Ac, and 500 yr for Am.

CONCLUSIONS

1. Rapid adsorption/uptake by biota in surface waters is predicted, based on the behaviour of the rare earth elements.

2. Remineralisation in deep water is also predicted.

3. Bacteria are possibly the most important scavenger of elements in the deep sea.

4. Bacteria are a possible mechanism for the dispersal of radionuclides from the site, but may carry material back to the margin.

5. The tentative prediction is for Pu to behave like Ce and Th, Am like La, and Ac like the light REE.

ACKNOWLEDGEMENTS

Thanks are extended to the officers and crew of RRS Discovery and Charles Darwin. Nicholas Rissler and Claude Lambert of the CNRS, Gif-sur-Yvette, who performed analyses of Station 10554 at the Laboratoire "Pierre-Süe" at Saclay, France, and to Ann Isley of the University of Rhode Island, USA, for analyses for Station 11287. We are particularly indebted to Pat Gwilliam, Les Wright, Dave Groman and other members of the IOS Engineering and Applied Physics groups for equipment development and support in the laboratory and at sea.

Thanks are also due to John Patching, Richard Jordan and Richard Lampitt for use of data.

This research has been carried out under contract for the Department of the Environment as part of its radioactive waste management research programme. The results will be used in the formulation of Government policy but, at this stage, do not necessarily represent Government policy.

REFERENCES

BACON, M.P. & ANDERSON, R.F. 1982 Distribution of thorium isotopes between dissolved and particulate forms in the deep sea. Journal of Geophysical Research, 87, 2045-2056.

BARTZ, R., ZANEVELD, J.R.V. & PAK, H. 1978 A transmissometer for profiling and moored observations in water. Proceedings of the Society of Photo-Optical Instrumentation Engineers, 160, 102-108.

BILLETT, D.M.S., LAMPITT, R.S., RICE, A.L. & MANTOURA, R.F.C. 1983 Seasonal sedimentation of phytoplankton to the deep-sea benthos. Nature, 302, 520-522.

BISHOP, J.K.B. 1986 The correction and suspended particulate matter calibration of Sea Tech transmissometer data. Deep-Sea Research, 33A, 121-134.

BREWER, P.G. & HAO, W.M. 1979 Oceanic elemental scavenging. pp.261-264 in, Chemical Modelling of Aqueous Systems, (ed. E.A. Jenne). New York: American Chemical Society. ACS Symposium Series, No. 93.

CANTRELL, K.J. & BYRNE, R.H. 1987 Rare earth element complexation by carbonate and oxalate ions. Geochimica et Cosmochimica Acta, 51, 597-605.

DEUSER, W.G., ROSS, E.H. & ANDERSON, R.F. 1981 Seasonality in the supply of sediment to the deep Sargasso Sea and implications for the rapid transfer of matter to the deep ocean. Deep-Sea Research, 28A, 495-505.

ELDERFIELD, H. & GREAVES, M.J. 1982 The rare earth elements in seawater. Nature, 298, 214-219.

HONJO, S. 1977 Biogenic carbonate particles in the ocean; do they dissolve in the water column? pp.269-293 in The Fate of Fossil Fuel CO_2 in the Oceans: (ed. N.R. Andersen & A. Malahoff). New York: Plenum Publishing Corp.

HONJO, S. 1978 Sedimentation of materials in the Sargasso Sea at a 5367m deep station. Journal of Marine Research, 38, 53-97.

HONJO, S. 1980 Material fluxes and modes of sedimentation in the mesopelagic and bathypelagic zones. Journal of Marine Research, 38, 53-97.

JICKELLS, T.D., DEUSER, W.G. & KNAP, A.H. 1984 The sedimentation rates of trace elements in the Sargasso Sea measured by sediment trap. Deep-Sea Research, 31A, 1169-1178.

LAMBERT, C.E., JEHANNO, C., SILVERBERG, N., BRUN-COTTAN, J.C. & CHESSELET, R. 1981 Log-normal distributions of suspended particles in the open ocean.
Journal of Marine Research, 39, 77-98.

LODER, T.C. & LISS, P.S. 1982 The role of organic matter in determining the surface charge of suspended particles in estuarine and oceanic water.
Thalassia Jugoslavica, 18, 433-447.

McCAVE, I.N. 1975 Vertical flux of particles in the ocean.
Deep-Sea Research, 22, 491-502.

McCAVE, I.N. 1984 Size spectra and aggregation of suspended particles in the deep ocean.
Deep-Sea Research, 31A, 329-352.

ROE, H.S.J. 1984 RRS Discovery Cruise 148, 21 May-12 June 1984.
Biological studies in the eastern North Atlantic (48°N-35°N) centred around King's Trough Flank (42°00'N, 21°30'W).
Institute of Oceanographic Sciences, Cruise Report, No. 163, 31pp.

ROESLER, H.J. & LANGE, H. 1972 Geochemical Tables.
Amsterdam: Elsevier Publishing Company, 468pp.

SAUNDERS, P.M. 1987 Currents, dispersion and light transmittance measurements on the Madeira Abyssal Plain. Final Report March 1987.
Institute of Oceanographic Sciences Deacon Laboratory, Report, No. 241, 55pp.

SCHINDLER, P.W. & STUMM, W. 1987 The surface chemistry of oxides, hydroxides and oxide minerals.
pp.83-110 in, Aquatic Surface Chemistry, (ed. W. Stumm).
New York: John Wiley & Sons, 520pp.

SIMPSON, W.R. 1984 RRS Discovery Cruise 147, 26 April-17 May 1984.
Biogeochemical fluxes in the NE Atlantic (42°N and 50°N transects)
Institute of Oceanographic Sciences, Cruise Report, No. 164, 40pp.

SIMPSON, W.R. 1987 RRS Discovery Cruise 159, 15 May-25 June 1986.
Biogeochemical flux studies in the NE Atlantic - GME, 26°N transect and TAG hydrothermal field.
Institute of Oceanographic Sciences Deacon Laboratory, Cruise Report, No. 193, 59pp.

SIMPSON, W.R., GWILLIAM, T.J.P., LAWFORD, V.A., FASHAM, M.J.R. & LEWIS, A.R. 1987 In-situ deep water particle sampler and real-time sensor package with data from the Madeira Abyssal Plain.
Deep-Sea Research, 34A, 1477-1497.

THOMSON, J. 1982 RRS Discovery Cruise 125, 30 January-25 February 1982.
Geochemical sampling over the Madeira/Cape Verde Abyssal Plains.
Institute of Oceanographic Sciences, Cruise Report, No. 125, 14pp.

WEAVER, P.P.E., BUCKLEY, D.E. & KUIJPERS, A. In press Sedimentological investigations of ESOPE cores from the Madeira Abyssal Plain. Report of the Marion Dufresne Cruise: (ed. R.T.E. Schuttenhelm). (in press).

WILSON, T.R.S. 1982 RRS Discovery Cruise 129, 22 May-22 June 1982. Geochemical sampling in the Tropical and Subtropical Eastern Atlantic. Institute of Oceanographic Sciences, Cruise Report, No. 138, [14pp].

WHITFIELD, M. & TURNER, D.R. 1979 Water-rock partition coefficients and the composition of seawater and river water. Nature, 278, 132-137.

WHITFIELD, M. & TURNER, D.R. 1981 Sea water as an electrochemical medium. pp.3-60 in, Marine Electrochemistry: a practical introduction, (ed. M. Whitfield & D. Jagner). Chichester: John Wiley & Sons Ltd., 529pp.

FIGURE CAPTIONS

Figure 1 Idealised difference distribution.

Figure 2 Cumulative number distribution: top line, surface water; bottom line, mid-water.

Figure 3 Work area on the Madeira Abyssal Plain.

Figure 4 Transmissometer mooring configuration.

Figure 5 Sediment trap mooring configurations.

Figure 6 Top - ship's record of DWPS cast Station 10554.
Right - CTD transmissometer cast, Station 8.

Figure 7 Mass concentration profiles, Stations 10554 and 11287.

Figure 8 Particulate concentration profiles of calcium, aluminium and iodine and equivalent calcite, clay and organic C mass concentrations, Station 10554 and Station 11287 (ng l^{-1}).

Figure 9 10 m above-bottom current: transmissometer mooring record and instrument drift.

Figure 10 Dry weight particle mass fluxes from the three sediment trap deployments.

Figure 11 Proportionality of major mineral phases in small particles.

Figure 12 Difference distributions of major particle types in the NE Atlantic (combined station and depth data): 10-100 μm particles.

Figure 13 Plankton community structure over the Madeira Abyssal Plain, May and July.

Figure 14 Coccolithophorid family distributions over the Madeira Abyssal Plain, May to July.

Figure 15 Coccolithophorid species distributions over the Madeira Abyssal Plain, May to July.

Figure 16 Enrichment factors of elements in the upper and deep ocean.

Figure 17 Electrophoretic mobilities of particles in the NE Atlantic.

Figure 18 Table of the elements based on predicted oxidation states in sea water and isoelectronic structure of outer shell.

Figure 19 Energy coefficients against elements in major oxidation states related to biogeochemical character.

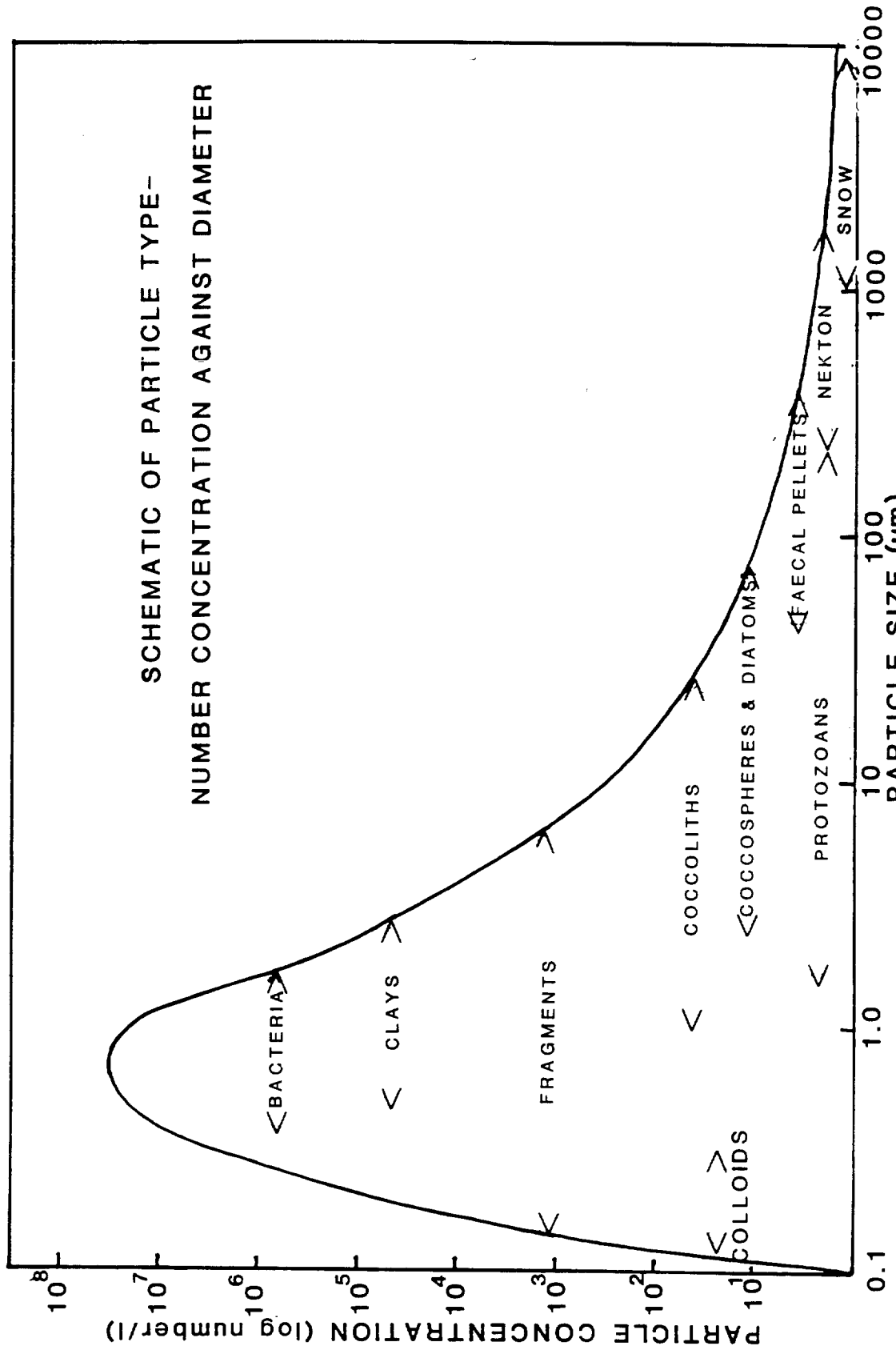

Figure 1 Idealised difference distribution

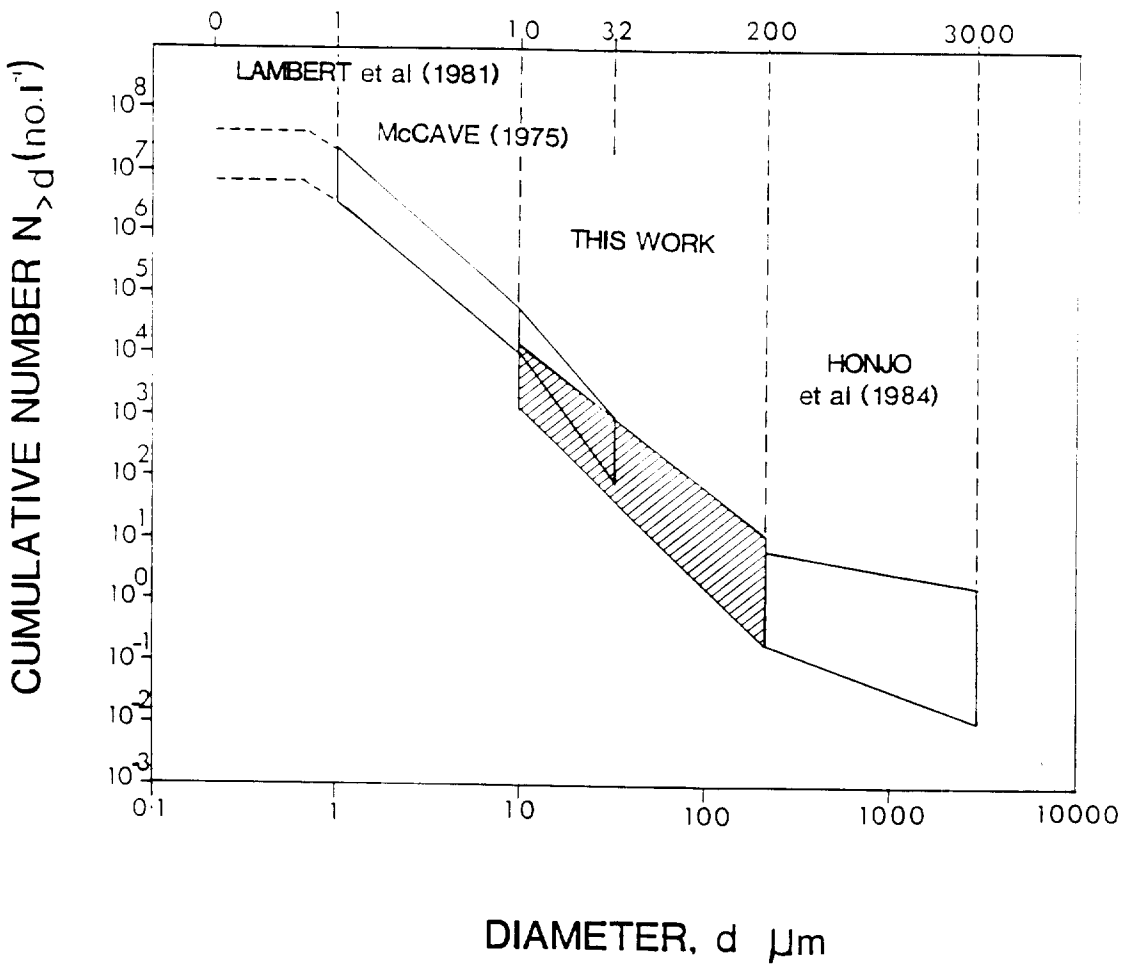

Figure 2 Cumulative number distribution - Top line surface water, bottom line midwater.

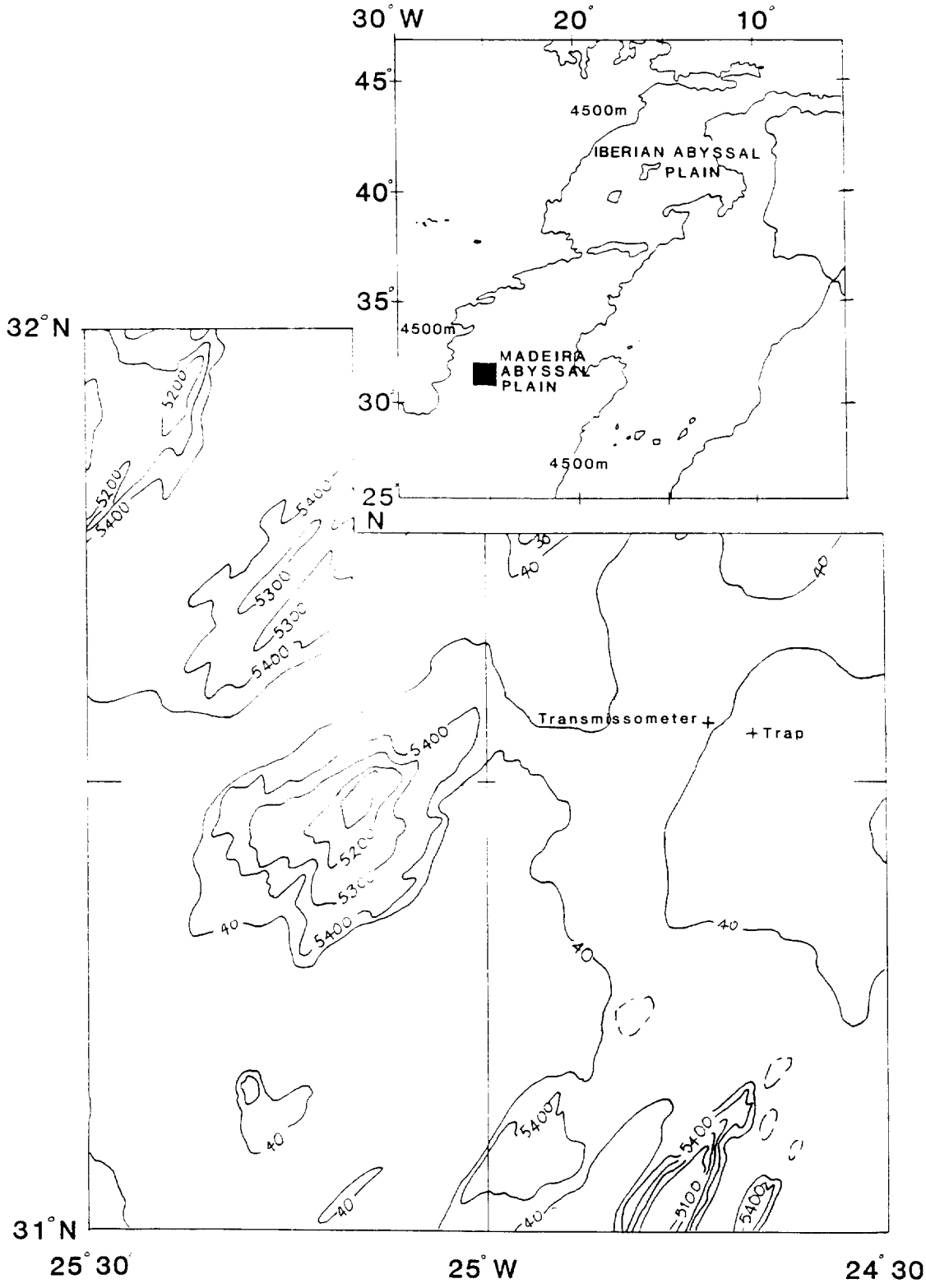

Figure 3 Work area on the Madeira Abyssal Plain

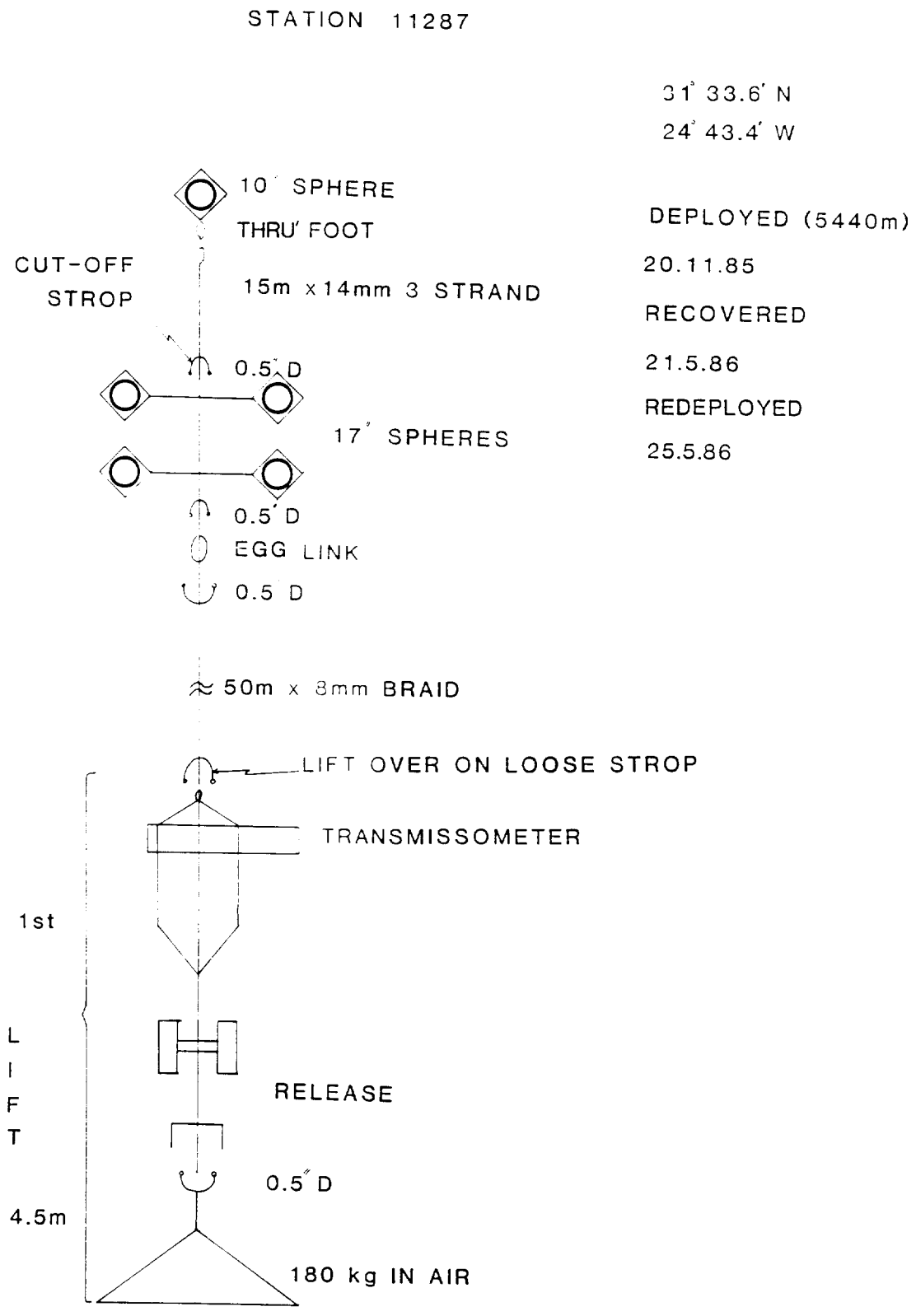

Figure 4 Transmissometer mooring configuration.

STATION 11287

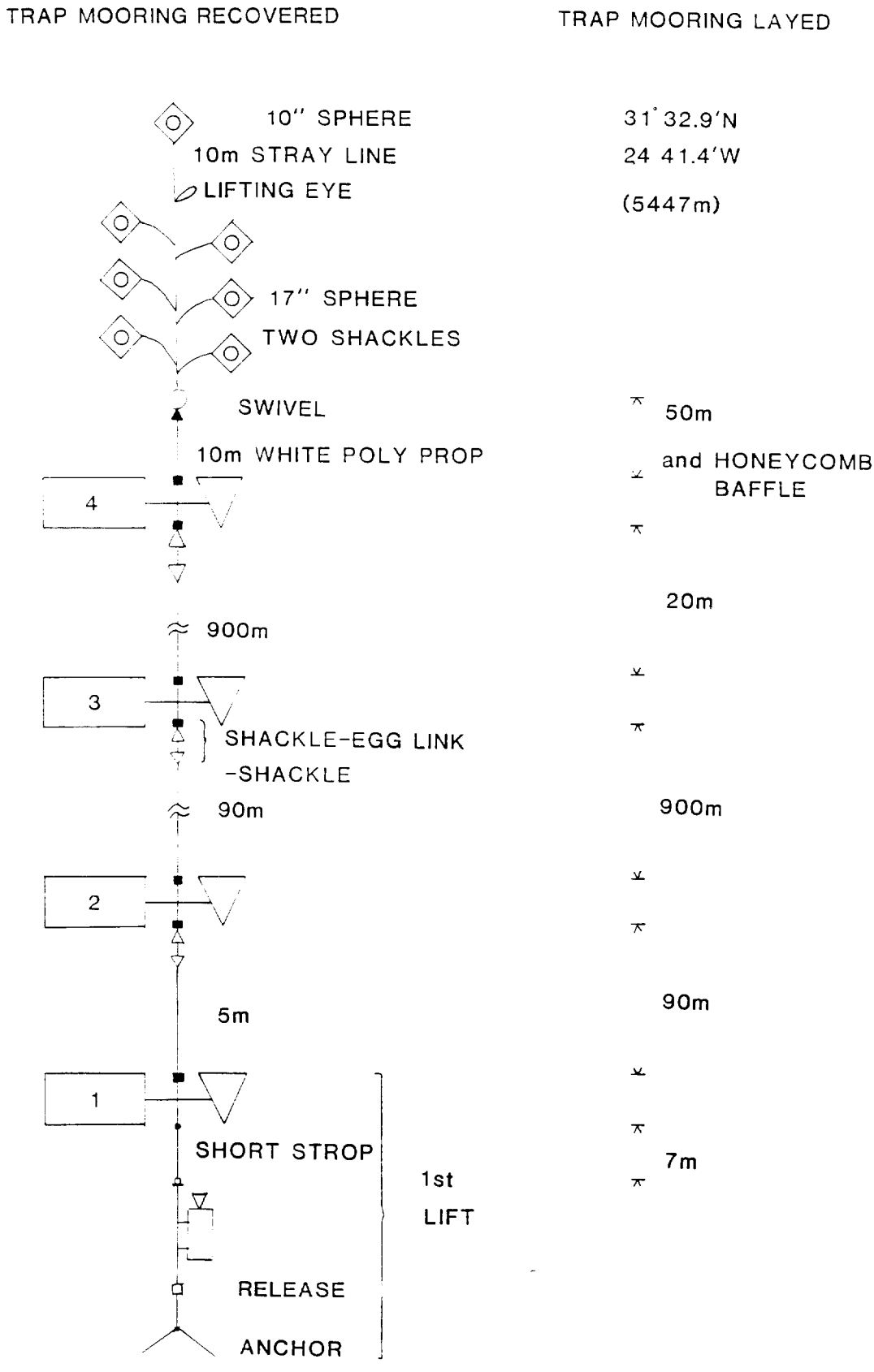

Figure 5 Sediment trap mooring configurations.

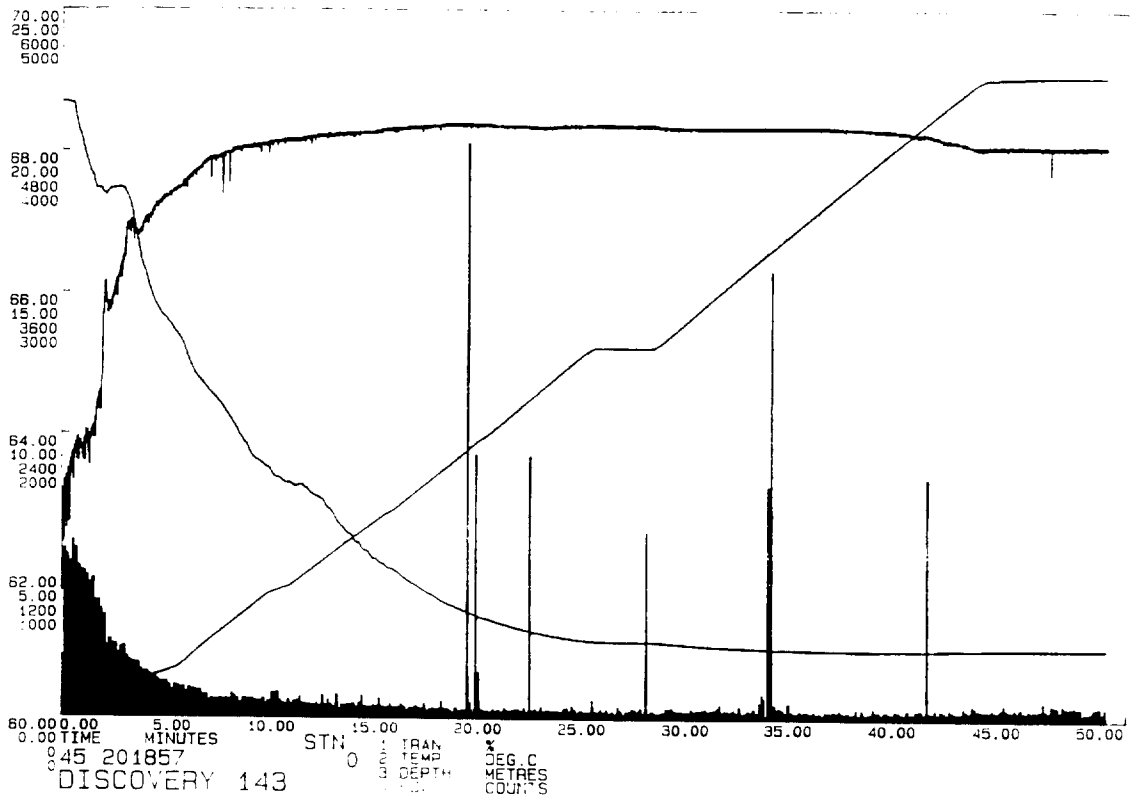

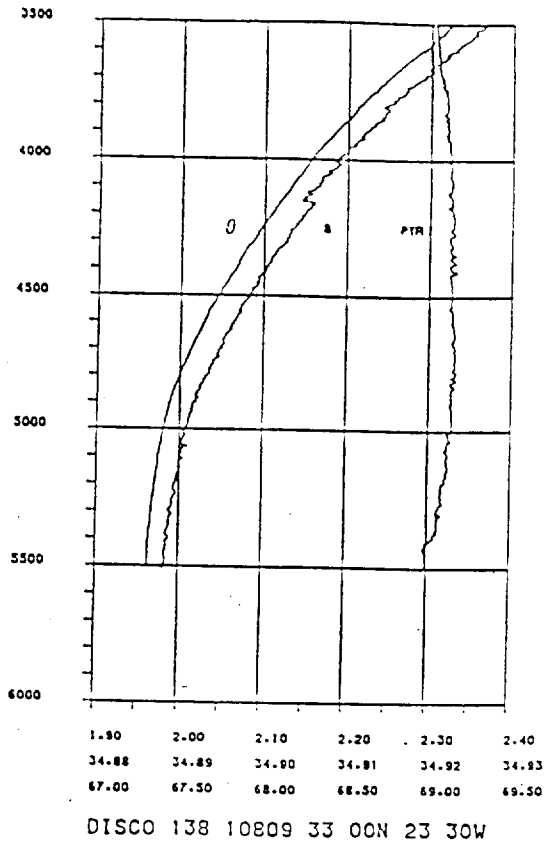

Figure 6 (Top) - ship's record of D.W.P.S. cast station 10554
(Right) CTD - transmissometer cast, station 8.

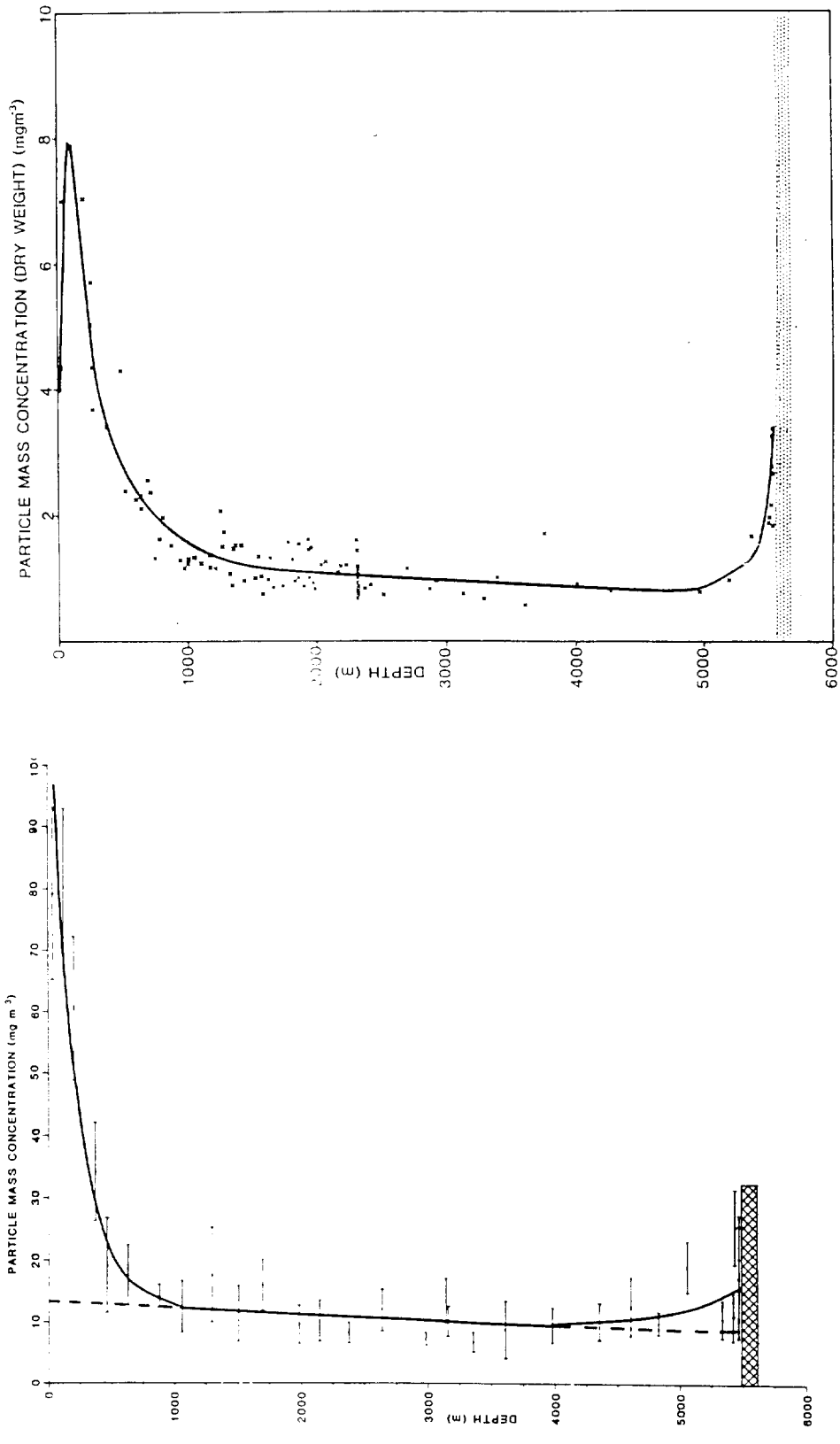

Figure 7 Mass concentration profiles, Stations 10554 and 11287.

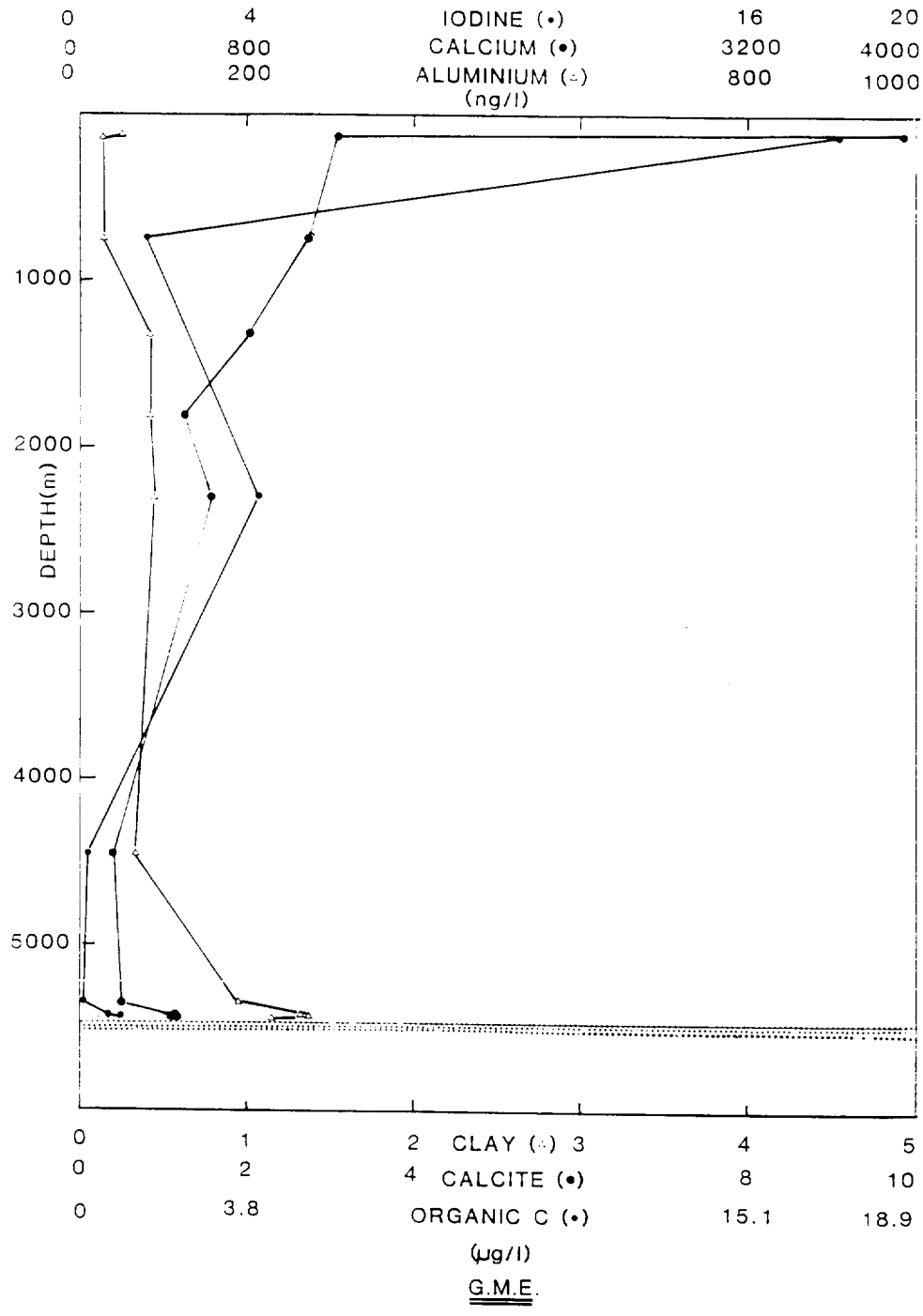

Figure 8 Particulate concentration profiles of calcium, aluminium and iodine and equivalent calcite, clay and organic C mass concentrations, Station 10554 and Station 11287 (ng l^{-1}).

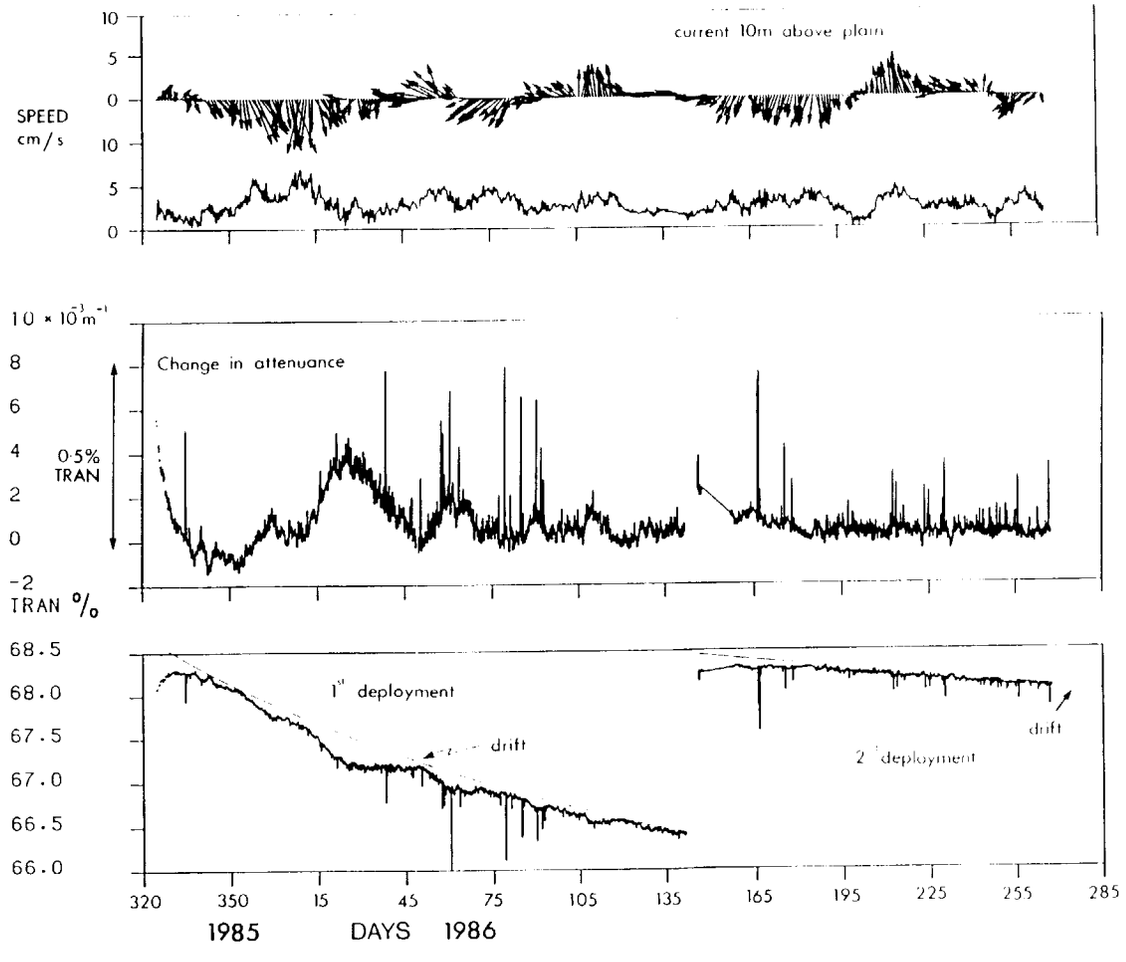

Figure 9 10 m above-bottom current; transmissometer mooring record and instrument drift.

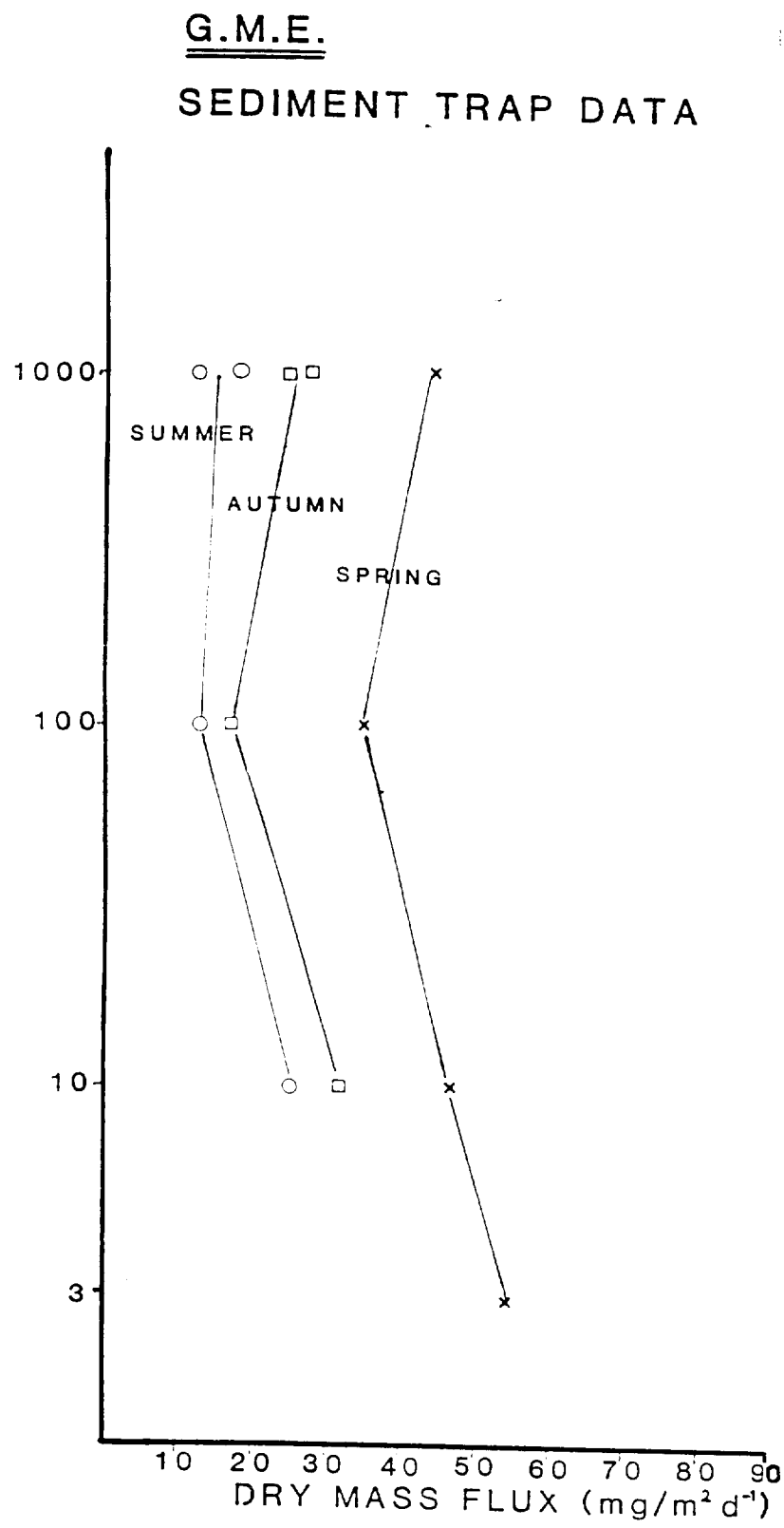

Figure 10 Dry weight particle mass fluxes from the three sediment trap deployments.

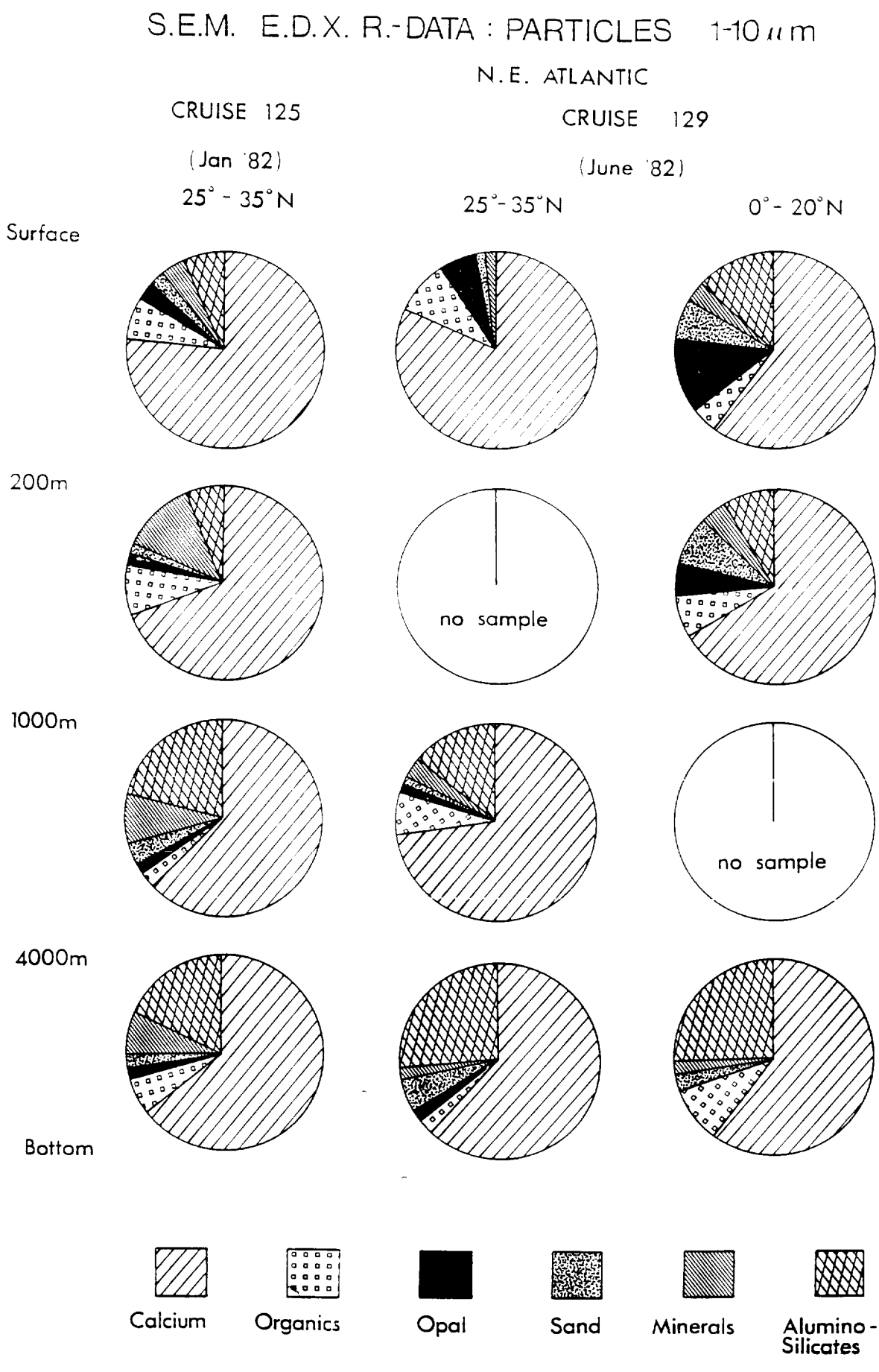

Figure 11 Proportionality of major mineral phases in small particles.

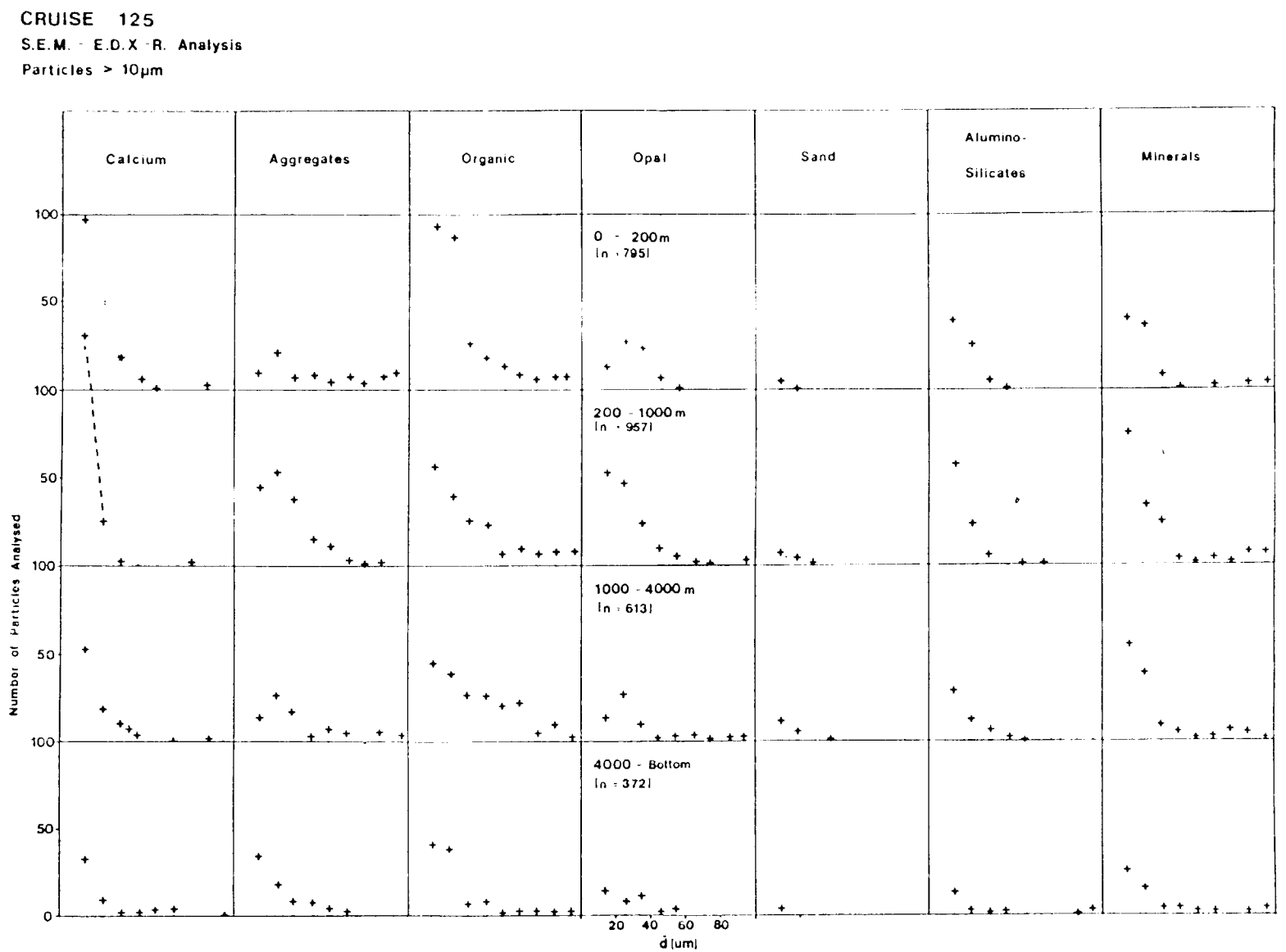

Figure 12 Difference distributions of major particle types in the N.E. Atlantic (combined station and depth data): 10 - 100µm particles.

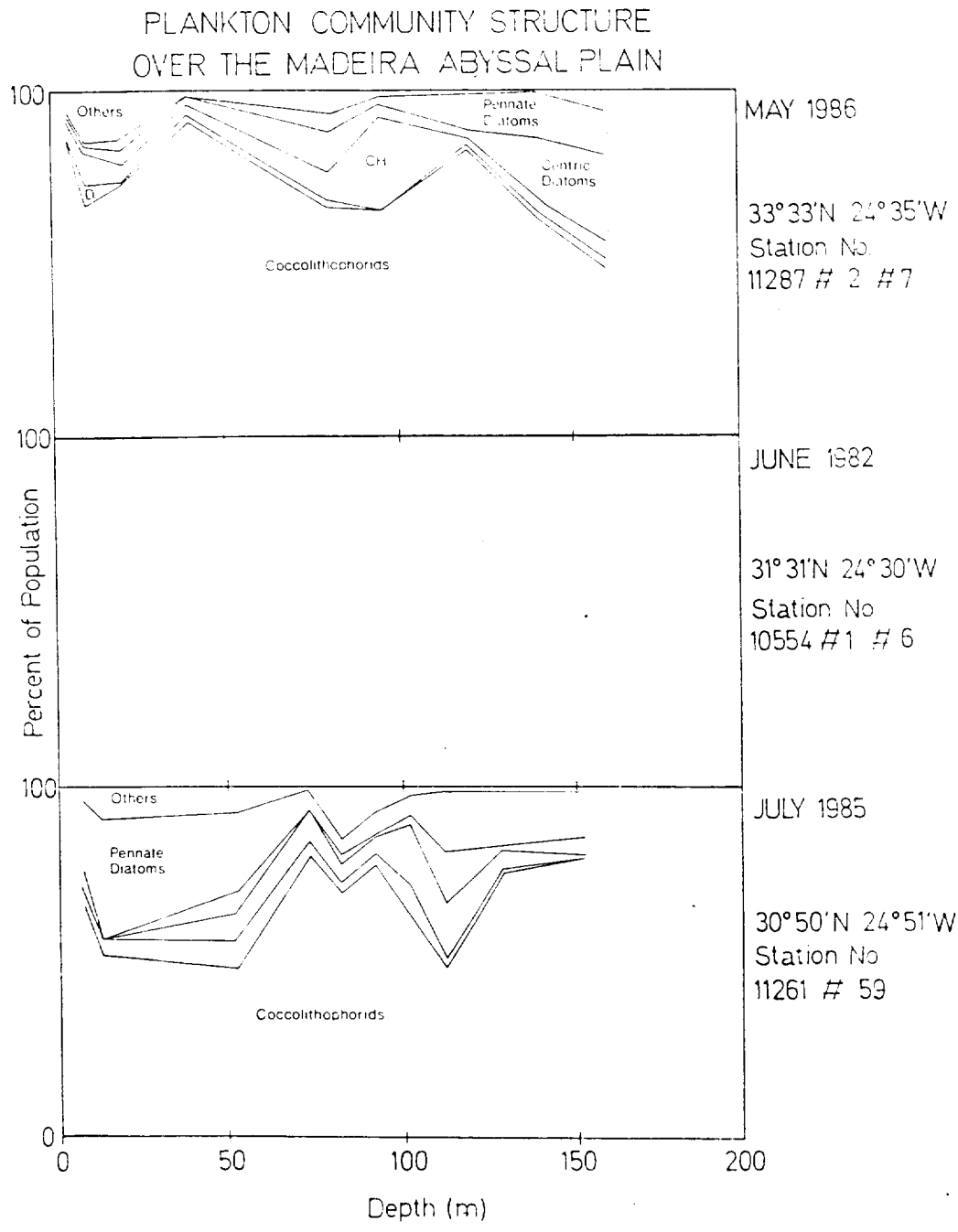
PLANKTON COMMUNITY STRUCTURE
OVER THE MADEIRA ABYSSAL PLAIN
100
Others
Pennate Diatoms
CH
Centric Diatoms
Coccolithophorids
MAY 1986
33°33'N 24°35'W
Station No.
11287 # 2 # 7
100
JUNE 1982
31°31'N 24°30'W
Station No
10554 # 1 # 6
Percent of Population
100
Others
Pennate Diatoms
Coccolithophorids
JULY 1985
30°50'N 24°51'W
Station No
11261 # 59
0
0
50
100
150
200
Depth (m)

Figure 13

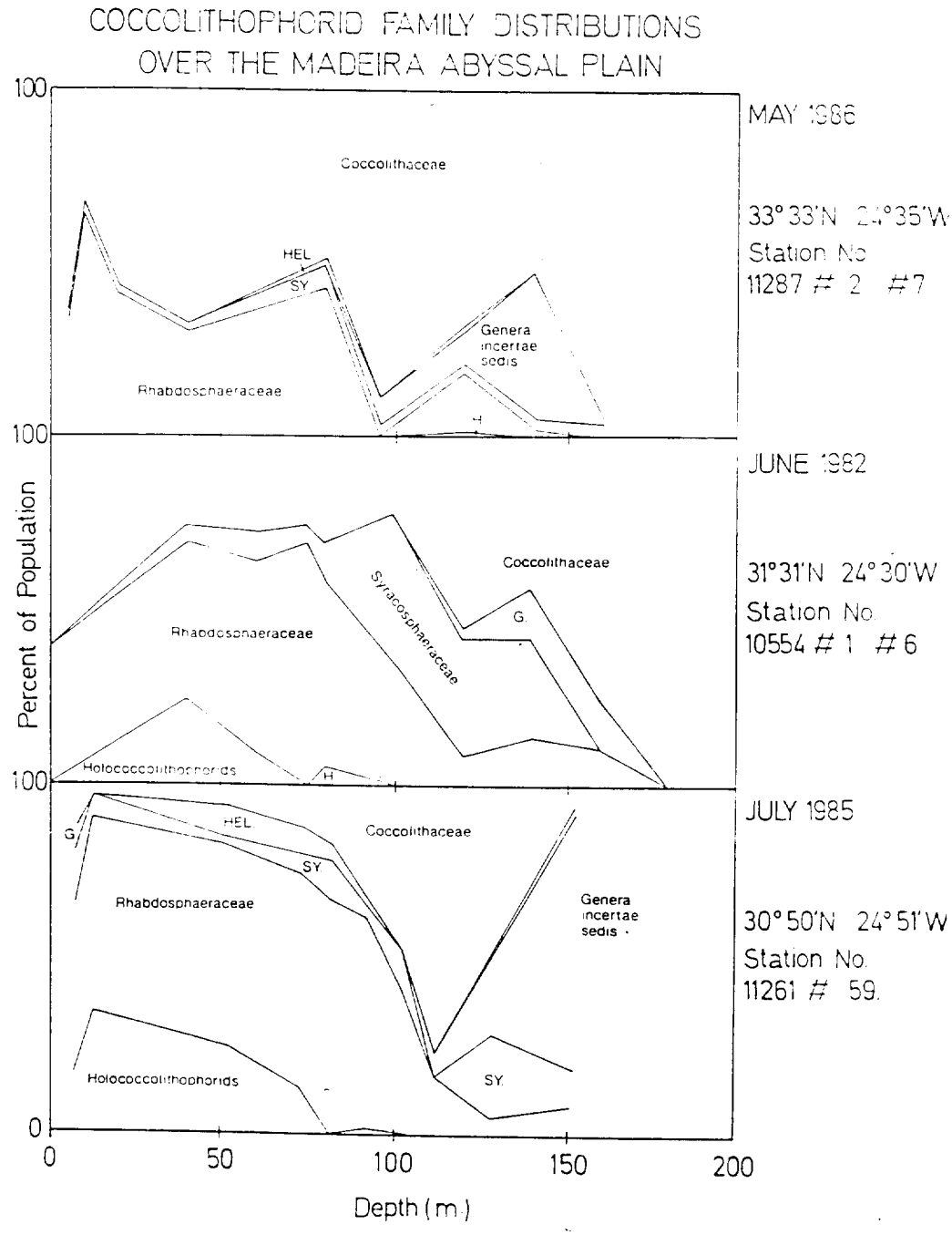
COCCOLITHOPHORID FAMILY DISTRIBUTIONS
OVER THE MADEIRA ABYSSAL PLAIN
MAY 1986
33°33'N 24°35'W
Station No
11287 # 2 #7
JUNE 1982
31°31'N 24°30'W
Station No
10554 # 1 #6
JULY 1985
30°50'N 24°51'W
Station No.
11261 # 59.
Coccolithaceae
HEL
SY
Genera incertae sedis
Rhabdosphaeraceae
H
G
Syracosphaeraceae
Holococcolithophorids
Percent of Population
100
0
0
50
100
150
200
Depth (m)

Figure 14

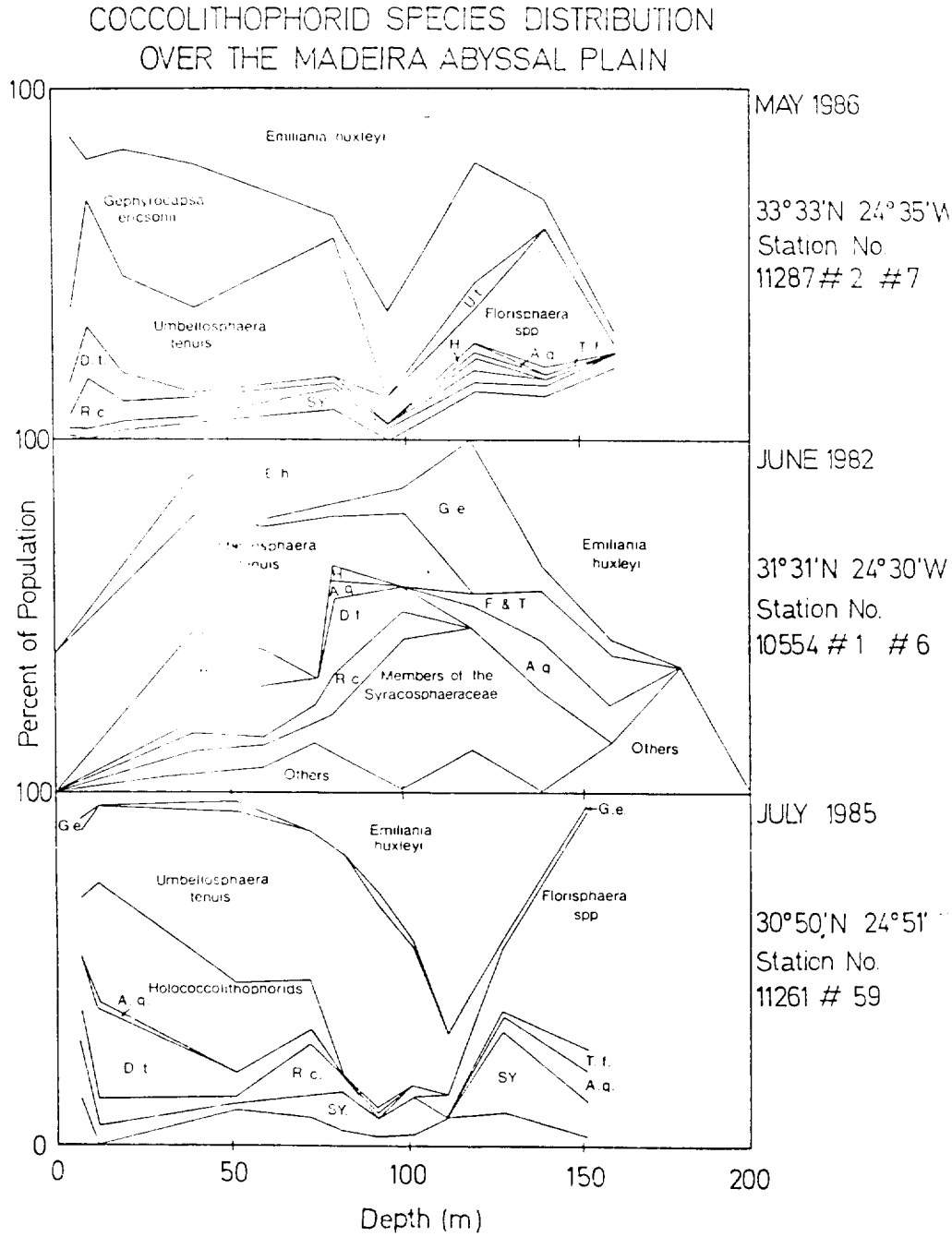
COCCOLITHOPHORID SPECIES DISTRIBUTION
OVER THE MADEIRA ABYSSAL PLAIN
MAY 1986
33°33'N 24°35'W
Station No.
11287 # 2 #7
JUNE 1982
31°31'N 24°30'W
Station No.
10554 # 1 #6
JULY 1985
30°50'N 24°51'
Station No.
11261 # 59
Emiliania huxleyi
Gephyrocapsa ericsonii
Umbellosphaera tenuis
Florisphaera spp
Members of the Syracosphaeraceae
Others
Holococcolithophorids
Percent of Population
Depth (m)
0
50
100
150
200

Figure 15

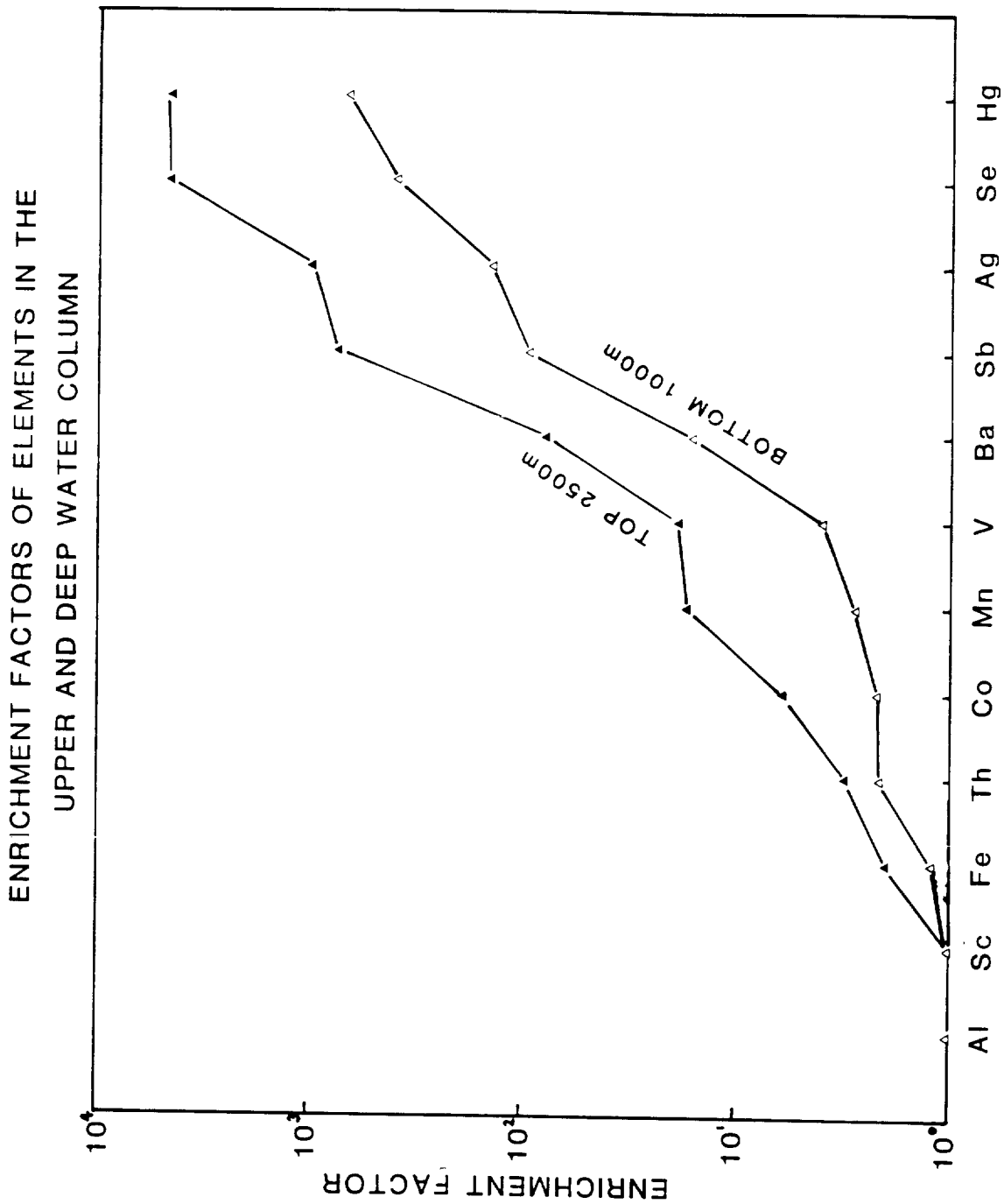
ENRICHMENT FACTORS OF ELEMENTS IN THE
UPPER AND DEEP WATER COLUMN
ENRICHMENT FACTOR
10^4
10^3
10^2
10^1
10^0
TOP 2500m
BOTTOM 10000m
Al Sc Fe Th Co Mn V Ba Sb Ag Se Hg
ELEMENT

Figure 16

ELECTROPHORETIC MOBILITIES OF PARTICLES IN THE NE ATLANTIC

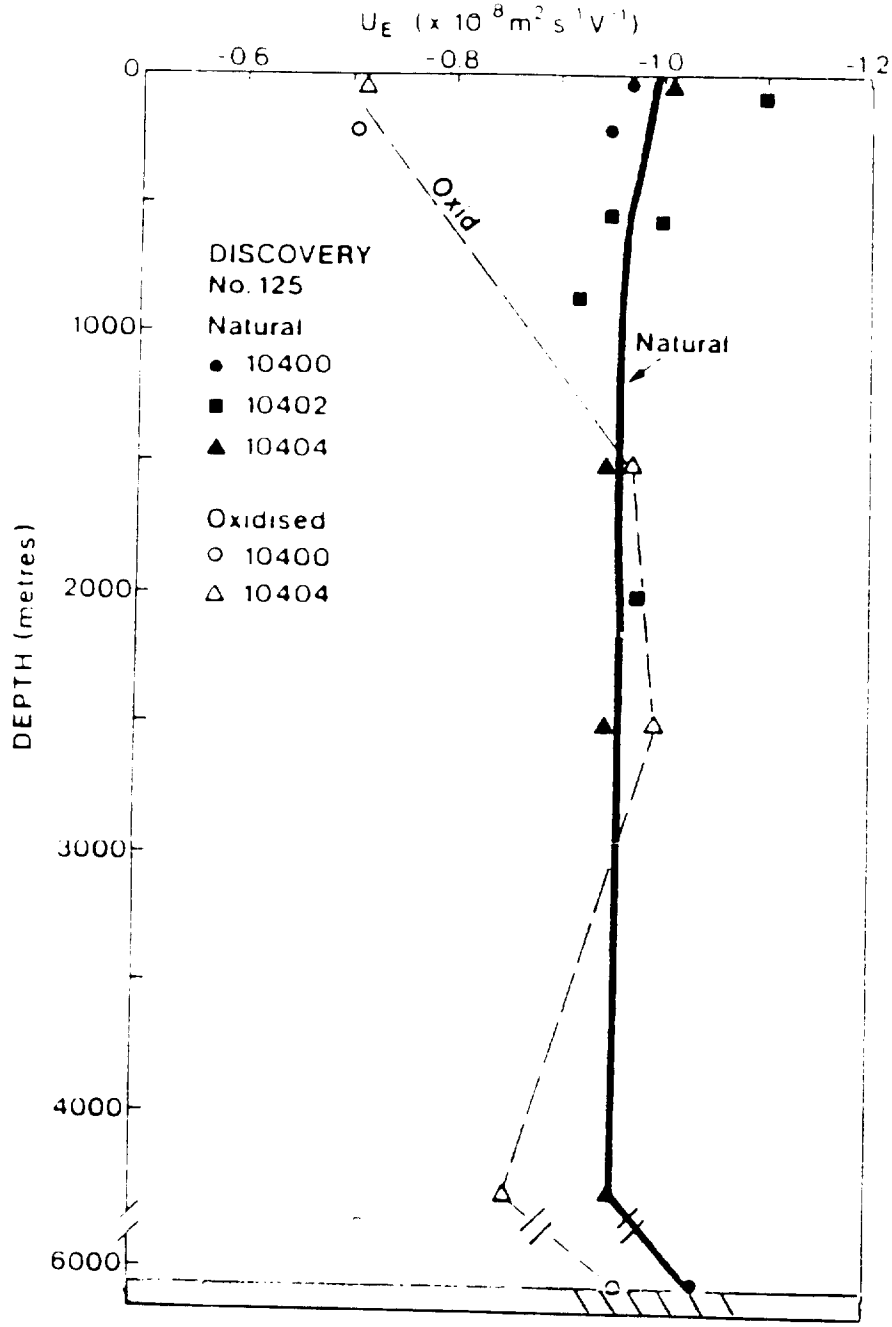

Figure 17

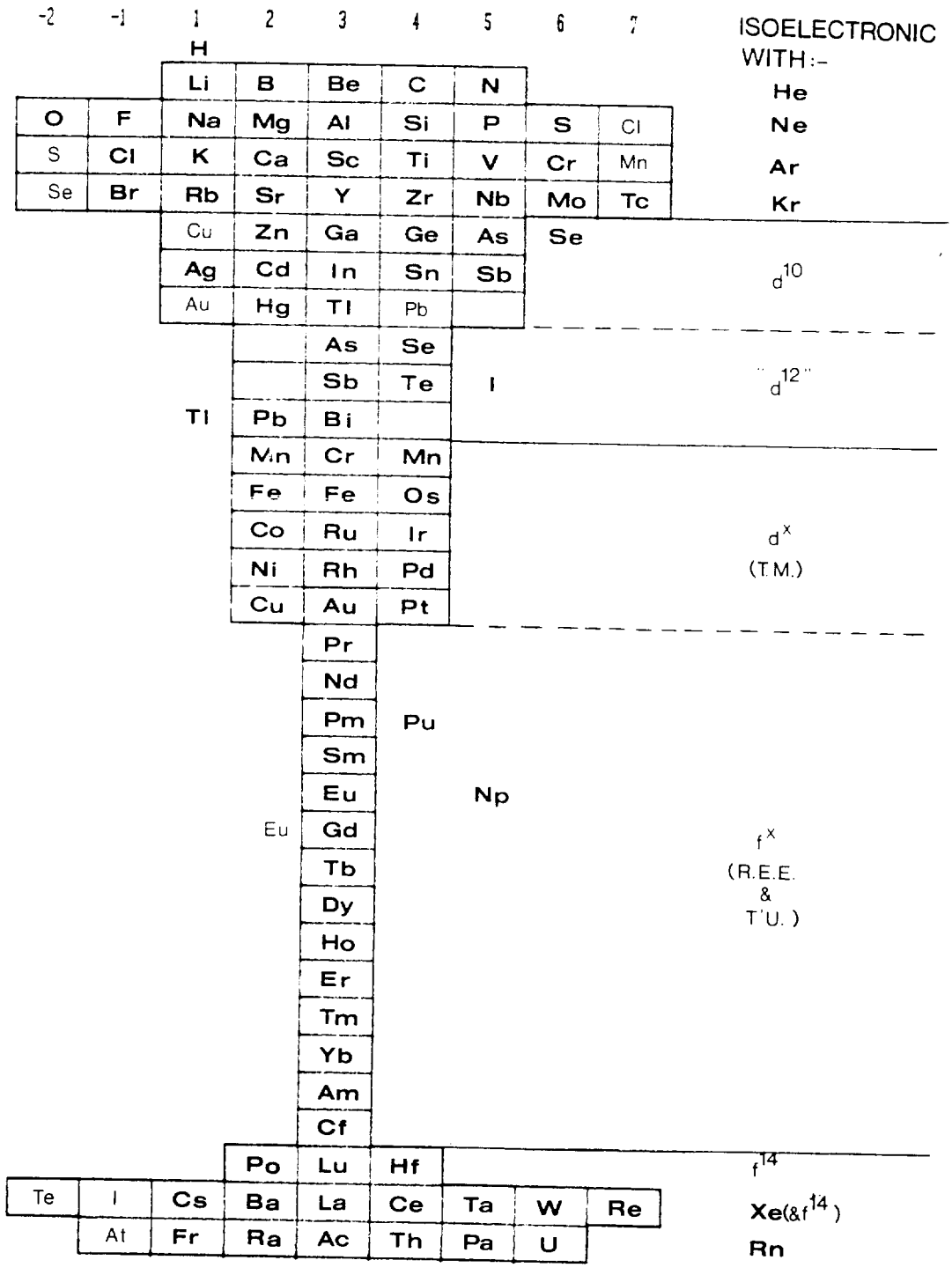

OXIDATION STATES OF ELEMENTS IN SCHEME RELATED TO THE OUTER ELECTRON SHELL

FIGURE 18.

FIGURE 19.
ENERGY COEFF. V ELEMENT

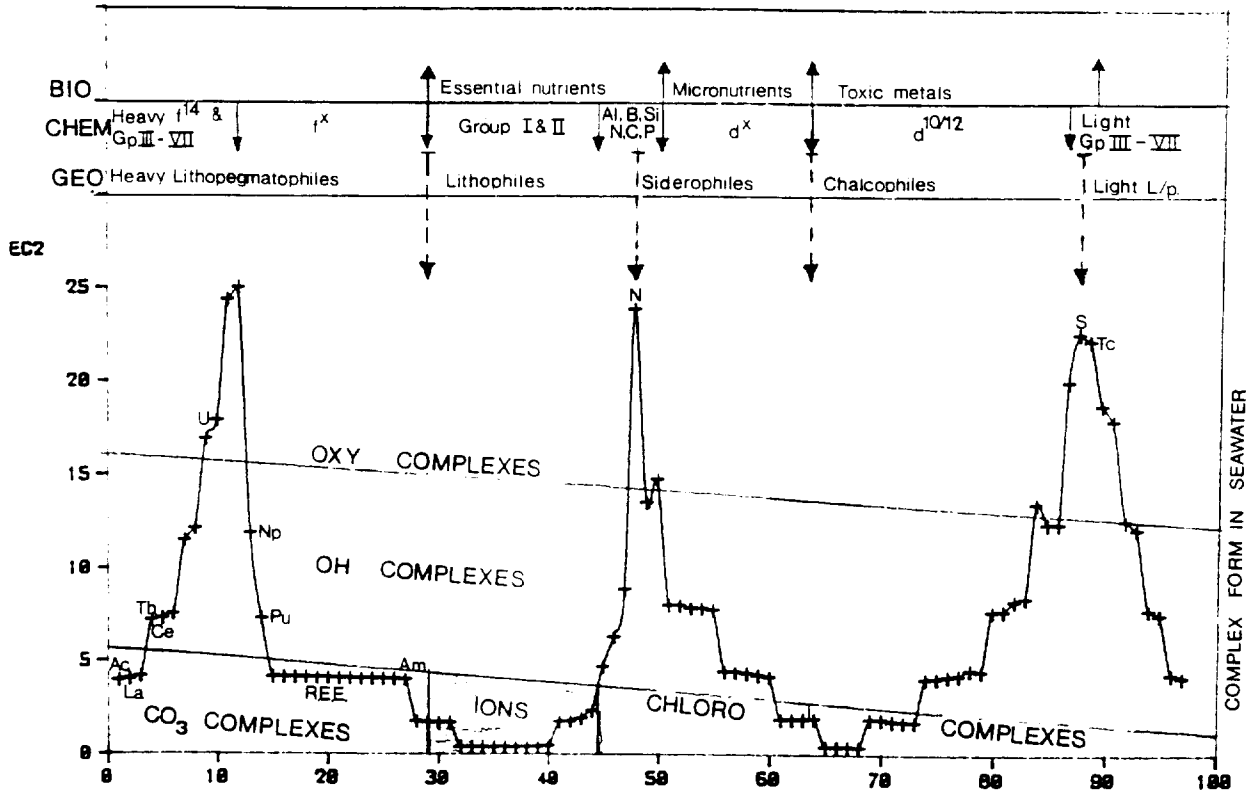

ELEMENT

REFNO	ELEMENT									
1	AC	21	GD	41	SR	61	MN	81	TE	
2	LA	22	EU	42	CA	62	FE	82	GE	
3	LU	23	SM	43	MG	63	CO	83	SE	
4	TH	24	PM	44	BE	64	NI	84	AS	
5	CE	25	ND	45	AL	65	CU	85	SB	
6	HF	26	PR	46	B	66	AG	86	I	
7	PA	27	AM	47	SI	67	AU	87	BE	
8	TA	28	EU	48	N	68	TL	88	S	
9	U	29	PO	49	C	69	CU	89	TC	
10	W	30	BA	50	P	70	ZN	90	CR	
11	AT	31	RA	51	MN	71	CD	91	MO	
12	RE	32	CS	52	OS	72	HG	92	V	
13	NP	33	FR	53	PT	73	PB	93	NB	
14	PU	34	BR	54	PD	74	BI	94	TI	
15	YB	35	CL	55	IR	75	TL	95	ZR	
16	TM	36	F	56	CR	76	IN	96	SC	
17	ER	37	RB	57	FE	77	SB	97	Y	
18	HO	38	K	58	RH	78	AS			
19	DY	39	NA	59	RU	79	GA			
20	TB	40	LI	60	AU	80	SN			

APPENDIX

Deep-Sea Research, Vol. 34, No. 8, pp. 1477–1497, 1987.
Printed in Great Britain.

0198-0149/87 $3.00 + 0.00
Pergamon Journals Ltd.

INSTRUMENTS AND METHODS

In situ deep water particle sampler and real-time sensor package with data from the Madeira Abyssal Plain

W. R. SIMPSON,* T. J. P. GWILLIAM,* V. A. LAWFORD,* M. J. R. FASHAM* and A. R. LEWIS*†

(*Received* 28 *July* 1986; *in revised form* 31 *December* 1986; *accepted* 7 *January* 1987)

Abstract—A deep water particle sampler was designed to measure physical variables in real time and collect particulate and water samples *in situ* with the view to furthering our understanding of biogeochemical cycles. Profiles of particulate concentration, particle size distribution (10–200 μm) and temperature against depth are taken on the outward and return casts to a maximum depth of 6000 m. Particle samples are collected by large volume filtration at four depths pre-selected on the basis of outward cast data. For metal analyses, 1 μm polycarbonate membranes are used, and glass fibre filters for organic analysis; larger particles may be collected by prefilters of any chosen mesh size.

Data presented from the Madeira Abyssal Plain illustrate the function of the instrument and the results are compared to those reported previously.

INTRODUCTION

SUSPENDED particles in ocean waters are primarily biogenic with a lesser contribution of non-biogenic minerals either transported from the continental masses or produced authigenically. The suspended particulate matter (SPM) holds the key to our understanding of the biogeochemical cycling of the elements. The removal of elements from solution, either by adsorption on to particle surfaces or by active biological uptake, is one step in their ultimate removal to sediments. During transit to sediments, the elements associated with the particles may be recycled many times via biological activity, dissolution, adsorption–desorption cycles, resuspension and post-depositional migration. Also the flux of particulate material can be accelerated by biological or physical aggregation (MCCAVE, 1984) or retarded by fragmentation (LERMAN, 1979). The general aspects of SPM in the oceans was reviewed recently (SIMPSON, 1982). Towards a fuller appreciation of how the system functions we need to know the rates of the processes and this involves the interrelationship of physical, chemical and biological controls. However, there is a basic constraint on the ease with which this can be achieved, that is, the low concentration of SPM in ocean waters, ranging from a few microgrammes per litre in

* Institute of Oceanographic Sciences, Brook Road, Wormley, Godalming, Surrey GU8 5UB, U.K.
† Research Vessel Base, No. 1 Dock, Barry, South Glamorgan, CF6 6UZ, U.K.

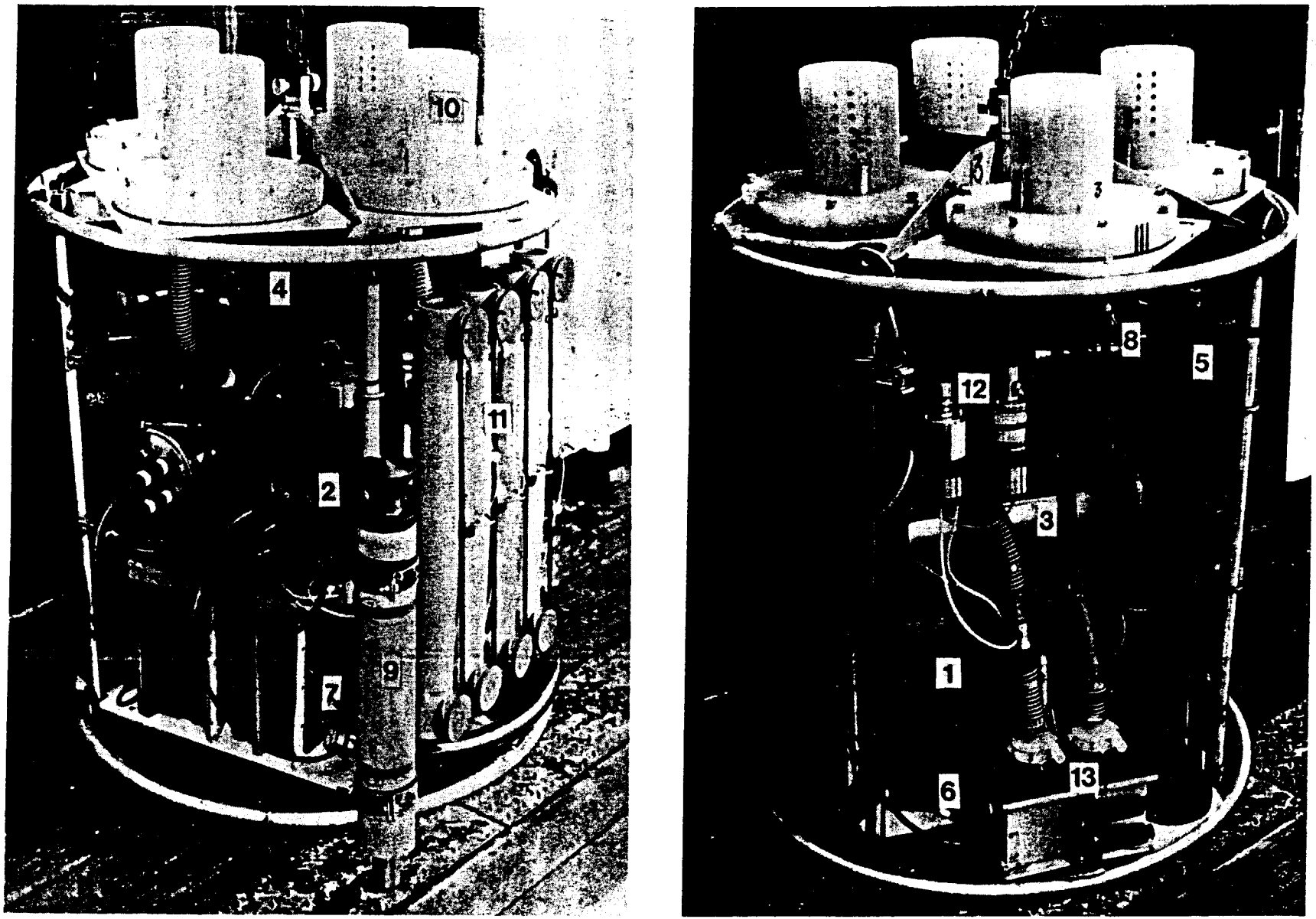

Fig. 1. The deep water particle sampler showing: 1. Battery packs. 2. Remote-control electronics tube. 3. Data transmission electronics tube. 4. Selector valve. 5. Transmissometer. 6. Pressure sensor. 7. Temperature sensor. 8. Particle counter. 9. Acoustic near-bottom echo sounder. 10. Filter stacks. 11. 2.5 l Go-Flo water samplers. 12. Pressure transducers. 13. Pumps and motor housing.

mid-water to a few hundred micrograms per litre in surface waters. *In situ*, large volume filtration (LVF) systems provide sufficient material for subsequent analysis; also, these instruments can act as vehicles for water samplers and *in situ* real-time sensors, e.g. conductivity, temperature, depth (CTD), particle concentration and particle size distribution.

Such a combination offers distinct advantages of *informed sampling*, taking samples of both particulates and water at depths based on information from the sensors, and *flexibility*, taking many samples at a number of depths on various stations over a short time period. Previously, LVF systems have not had this facility (LAIRD *et al.*, 1967; SPENCER and SACHS, 1970; BEER *et al.*, 1974; BISHOP and EDMOND, 1976; KRISHNASWAMI *et al.*, 1976; BISHOP *et al.*, 1980) but they have proved their versatility in radiotracer studies (e.g. BACON and ANDERSON, 1982) and major element fluxes in surface and intermediate waters (e.g. BISHOP *et al.*, 1980). With the proper precautions in clean handling techniques, these systems can also be applied to problems relating to trace element chemistry and, since the material is fresh, to the chemistry of labile as well as refractory organics.

A disadvantage of LVF is that samples are collected over minutes to hours, thus providing a "snap-shot" record that cannot show changes in particle composition, concentration or fluxes integrated over time as obtained by time-series sediment traps. However, problems of collection efficiency and sample preservation with traps have not been totally solved as yet. By LVF and particle counting, fluxes can be derived by models based on size distribution, density and water structure data (MCCAVE, 1975, 1984). In essence, pumps and traps complement each other; the former allowing a better understanding of the processes, the latter more suited to long-term flux evaluation.

The instrument described here was designed, first, to give real-time information, both on the physical structure of the water column under study and also the concentration and size distribution of the SPM and, second, to collect sufficient quantities of SPM by LVF ($1\ m^{-3}\ h^{-1}$) for subsequent chemical and morphological analysis. The sampling depths were chosen based on information obtained from the sensors on the outward cast. By combining the results, the data may be used to model fluxes of particulate material and the associated elements.

Since the system is new, the discussion centres on validation of the results in terms of sampling accuracy, as indicated by the chemical results, and by comparison of the particle counter data with attenuation coefficient against particle volume measurements and also with other particle size distribution work on open ocean samples. The station described was worked on R.R.S. *Discovery* Cruise 129 (Sta. 10554) at 31°29′N, 24°28′ in June 1983.

INSTRUMENTATION

The overall dimensions of the instrument (Fig. 1) are 1 m diameter, 1.1 m in height, weighing 450 kg in air and 250 kg in water. The instrument is lowered on a 10 mm Rochester conducting cable (9.2 Ω/100 m resistance and 5900 kg breaking strain). Casts are run at a maximum of $1\ m\ s^{-1}$, which maintains a working safety factor of 2.5 and to a maximum depth of operation of 6000 m within 10 m of the sea floor.

The following description will be given in three parts: the filtration system, the sensors, the data handling at sea and in the laboratory. Table 1 presents a summary of the main technical specifications.

Table 1. Summary of technical specifications

(a) Mechanics

Maximum flow available: 2480 l h^{-1}
With filters: 1000+ l h^{-1} *in situ*

Pumps	Austin centrifugal (polypropylene).
Motors	Printed motors G9M4 (24 V) in pressure-balanced housing.
Power	Chloride Cyclon lead-acid paste (5 Ah) 48 per pack in four units of 12 = 24 V (15 Ah). Pressure balanced.
Filters	Nuclepore polycarbonate (1 μm), Estal polyester (≥30 μm).
Volume meters	Kent mechanical positive displacement (1 part in 1000).
Selector valve	Rotary (cone-shaped) built in-house.
Water samplers	General Oceanics Go-Flo bottles (2.5 l).

(b) Sensors

		Range	Accuracy	Resolution
Temperature	Pt resistance thermometer	0–20°C	±0.005°C	0.002°C
Pressure	Strain gauge	6000 m	±4 m	0.05 m
Transmissometer	Seatech 1 m folded	0–100%	±0.5%	0.02%
Flow meters	Appleby-Ireland pressure transducer			
	(a) Venturi	0.3–3.0 m ^{3} h^{-1}	±5%	20 l h^{-1}
	(b) Particle cell	0.3–3.0 l min^{-1}	±5%	20 ml min^{-1}
Height off-bottom	35 kHz Acoustic sensor	9–256 m off	–	1 m
Particle counter	Light blockage principle	10–465 μm in 16 channels		

(c) Data processing

From sensors	Voltage or frequency to b.c.d. 8-bit words.
Transmission	FSK line signal $3\frac{1}{3}/6\frac{2}{3}$ kHz (≡ "0" and "1").
Demodulator	IOS FSK or Neil-Brown CTD deck unit.
Displays (raw data)	CTD unit, purpose-built unit and BBC microcomputer.
Computer	PDP 11/34 run under RSX 11M with sampling software in RTL/2, processing software in C and FORTRAN IV.
Display	Tektronix, H.P. graphics terminals plus printers and plotters.

The filtration system

Filter stacks. The design is shown in Fig. 2. The units were turned from nylon and crush between the top and base plate made with stainless steel nuts and bolts. A spiral groove was cut into the filter support plate and 2 mm holes drilled every 5 cm on the spiral, to provide even flow through the filters. The "top-hat" arrangement provided seal on the prefilter but its main function was to prevent both wash-off of material during passage through the water column and contamination of the sample.

A prefilter (142 mm diameter, Estal polyester >30 μm porosity) could be included in the stack to provide *in situ* fractionation of the robust larger particles. For metal analyses Nuclepore polycarbonate membranes of 1 μm porosity were used. For full elemental analyses it was estimated that the minimum amount of material required was 2 mg dry weight, equivalent to filtering 1 m^3 of water at the particle minimum. This volume was achieved in <1 h with 293 mm diameter, 1 μm membranes. The system can equally be applied to the study of the organic chemistry of particulates by using glass fibre filters (Whatman GFC or GFF).

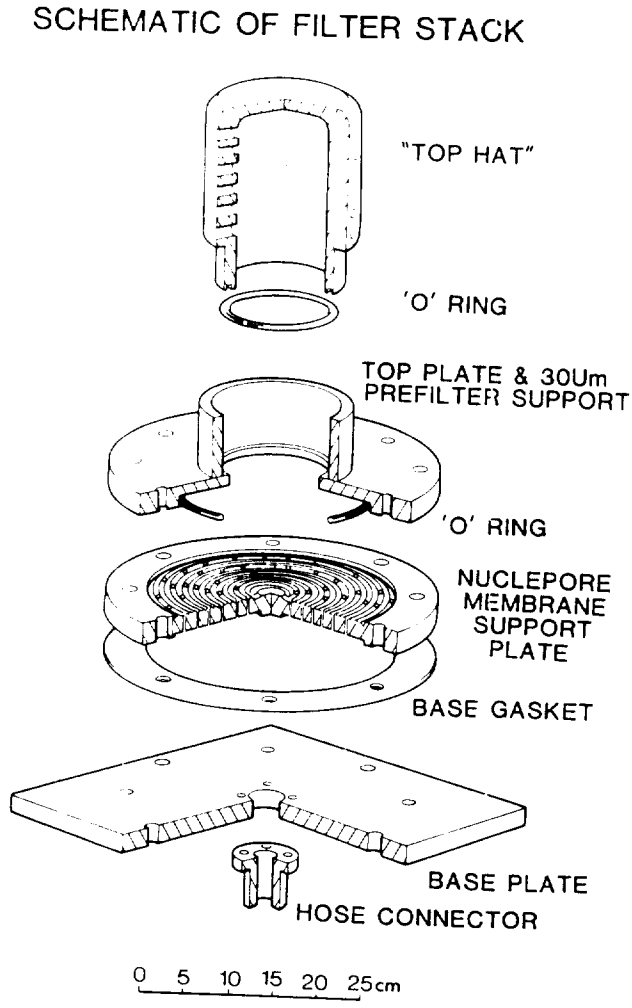

Fig. 2. A schematic of a filter stack.

Pumps and motors. A disc-type armature DC motor (G9M4 Printed Motors) that offered compactness, low drag armature and good efficiency was coupled to a polypropylene centrifugal pump (Austin). The motor was contained in a pressure-balanced plastic housing filled with liquid paraffin which has low viscosity and high electrical impedance. A seal around the drive shaft prevented seawater entering the box. Though the liquid drag decreased the efficiency of the motor, the better cooling allowed the use of a small motor driven at increased power rating (Fig. 3). Checks for carbonization were made during routine maintenance but after 200 h running at ambient pressures between 400 and 600 bars the wear on the bearings and brushes was slight.

The pump gave a maximum head of 10 m and the power requirement was reasonably constant at all flows with a maximum flow available of 2480 l h^{-1} (Fig. 3).

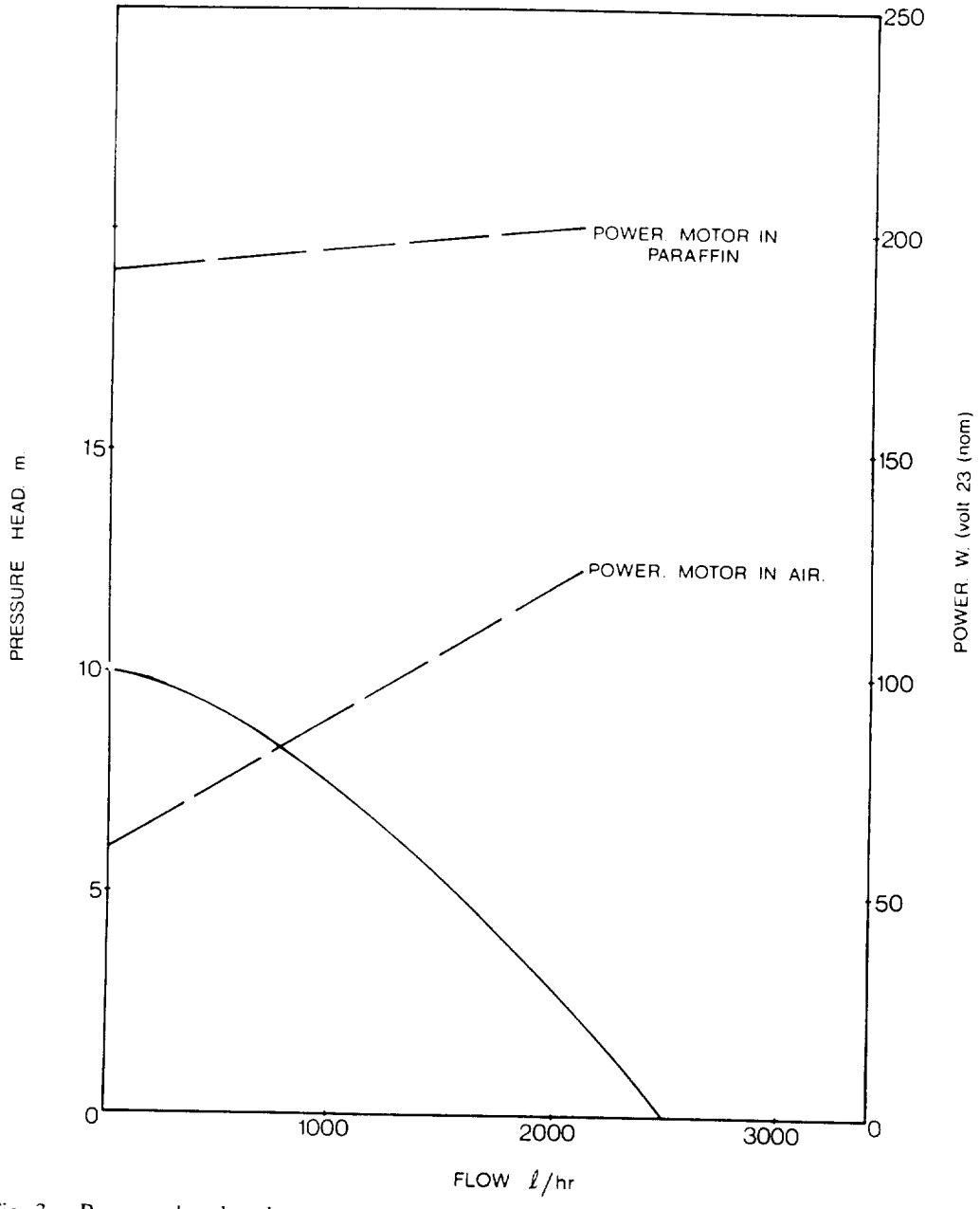

Fig. 3. Pressure head and power output on the motor and centrifugal pump run in paraffin and in air against flow rate.

Power. With a current demand of 20 A from a 24 V supply for the motor, it wa decided that the instrument should carry its own energy source. A close-wound lea plate and paste electrolyte cell was chosen in preference to lead-acid accumulators tha are difficult to handle at sea. Cells with a capacity of 5 Ah and 27 Wh kg^{-1} were use (Chloride Cyclon X001). There was an advantage in having the cells pressure balanced t allow light weight and inexpensive packaging. To test performance the outer casing of cell was removed, two holes drilled into the top of the inner polypropylene case an transformer oil injected into the cell to fill the air space. A normal cell at atmospheri pressure was compared to the modified cell at 600 bar over 10 identical charge–discharg cycles using a 1 Ω load. There were no large adverse effects over this number of cycle (Fig. 4). Mentor oil-filled cells showed less capacity drop than cells filled with othe liquids although liquid paraffin was only marginally worse.

Pressure balanced fibre glass boxes (34.5 × 34.5 × 9 cm) were made to hold 48 cells The cells were connected into four units of 12 in each box to supply 24 V (15 Ah) to th motor. Diodes were fitted to allow for the even discharge of power between units. Eacl box was fitted with a Perspex lid and the seal provided with screws and Selastic. Tw valves for pumping oil into the boxes, pressure balancing and gas pressure release o recharging were necessary. Six such boxes provided 6-h filtration time for one cast.

Flow meters. The essential requirements were accuracy, small resistance to flow an low power consumption.

A Venturi restriction above the pump inlet coupled to a modified pressure transduce of the LVDT type (Appleby and Ireland) was used for monitoring the flow rate in real time. This operated between 300 and 3000 l h^{-1} to ±5% accuracy. For greater accuracy

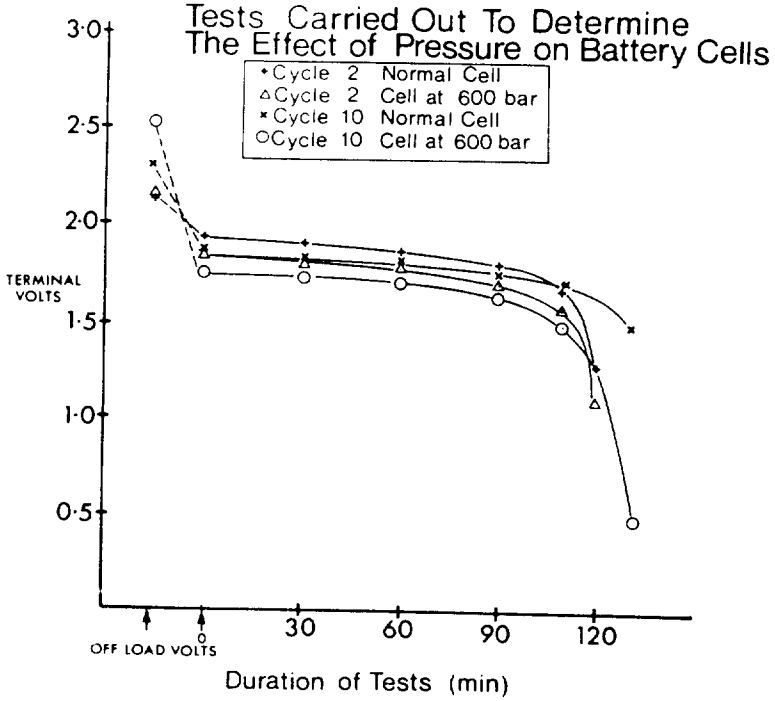

Fig. 4. Battery output vs discharge rate at atmospheric pressure and 600 bars after 2 and 10 discharge cycles.

the total volumes filtered were recorded by Kent mechanical positive displacement flow meters (accurate to one part in a thousand) fitted in-line between each stack and the selector valve.

Selector valve. The selector valve (Fig. 5) was designed to direct water flow through any of the four filter stacks. A motor and gear box supplied the torque to a spindle connected to a frustrum-shaped stainless steel valve. The valve had a 27 mm L-shaped hole through bottom to side. The filters were selected by rotation of the valve after direct command from the ship (see below). Positive identification of the position of an open valve port was made with reed switches activated by a magnet attached to the valve shaft. The binary-coded decimal (bcd) output information was transmitted and displayed on the shipboard display unit. A rotary solenoid was tried in the original instrument but was found to be unreliable.

Water samplers. Four General Oceanics water samplers were used on the rig (either 2.5 l Go-Flo samplers or 1.2 l Niskin bottles with reversing thermometer cages). Bottles were cocked as in normal operation, but held under tension by stainless steel springs coupled through a 10-Ω resistor. The bottles were fired by passing sufficient current to blow the resistor and hence close the bottle, the operation being controlled from the ship.

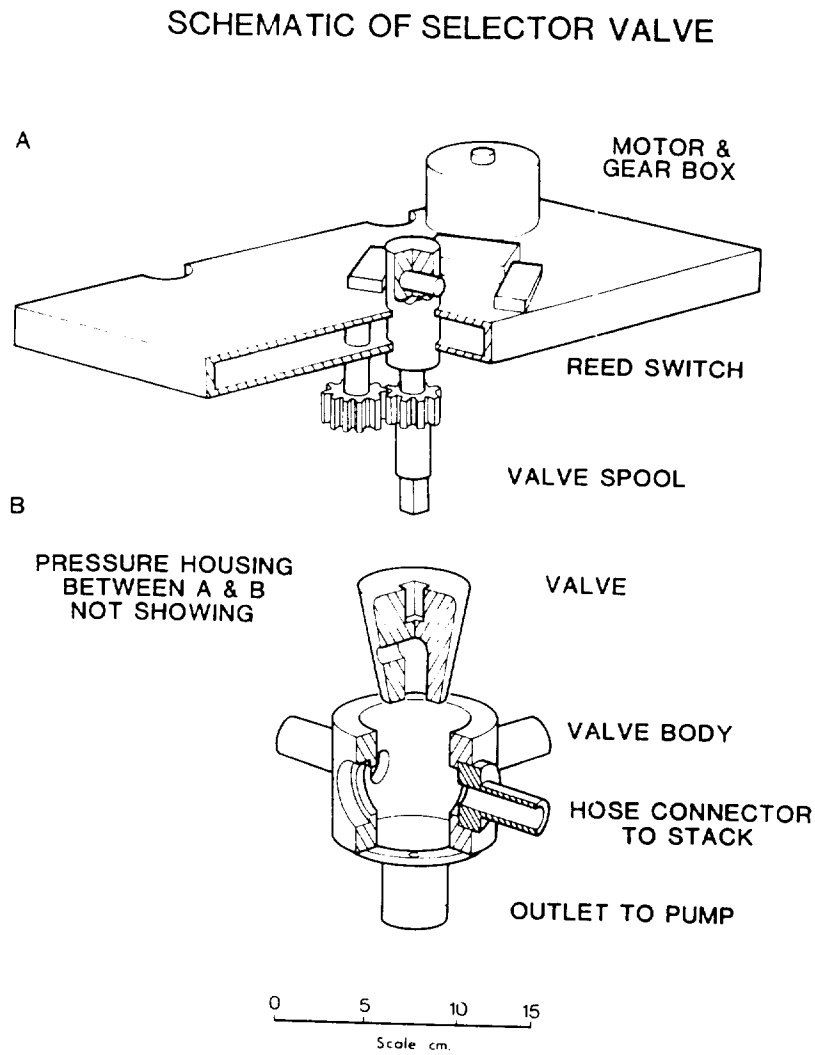

Fig. 5. Schematic of selector valve.

Remote command and control of functions. This system had three functions: to switch the pump motors on and off; to fire the water bottles; and to turn the filter selector valve. On command, the deck receiver equipment was isolated and a pre-selected binary code generated and transmitted as pulse position modulations signals down the cable to the receiver on the instrument. So that spurious signals did not interfere with the instrument, two consecutive identical transmissions were necessary to carry out the function desired. The signal decoded on the receiver electronics and the resultant number selected one of the required functions.

The sensors

With the emphasis on particulates, an optical particle counter and transmissometer were included in the instrument package. The counter constitutes a new *in situ* oceanographic instrument that effectively counts particles in the range 10–200 μm (see below). Former *in situ* counters have used the impedance principle and operated only in surface waters (MADDUX and KANWISHER, 1965; BOYD and JOHNSON, 1969; BROWN, 1977). Recently, HONJO *et al.* (1984) have described a photographic instrument for concentration estimates of particles >200 μm.

As mentioned above, the data from the sensors greatly enhance the sampling strategy for filtration, e.g. surface particle maximum, midwater minimum and nepheloid layer. Water and particle structure can be related and simple treatment of the particle counter data, assuming equivalent sphere diameters and density distribution, leads to estimates of particle volume, mass and flux for the size range measured.

Temperature, pressure and conductivity. The platinum resistance thermometer measured temperature over the range 0–20°C with an accuracy of ±0.005°C and resolution of 0.002°C. The strain gauge pressure sensor measured down to 6000 m with an accuracy of ±4 m and resolution of 0.6 m. Both operated with 1 s sampling with output frequency in the range 800–2000 Hz. For the station described below, conductivity measurements were taken on a separate cast using a Neil-Brown CTD. A prototype sensor based on a Beckman three-terminal conductivity cell is to be tested.

Particle concentration and size distribution. A Sea Tech Inc. 1 m folded beam transmissometer was used to monitor particle concentration (BARTZ *et al.*, 1978). The wavelength of operation was 660 nm so that the attenuation of light due to the suspended particles was measured with no interference from dissolved organic matter. A 10 V supply was required to provide a 100 mW power and the output ranged from 0 to 4.5 V, equivalent to 0–90% light attenuation in water. The air calibration was checked before deployment, and windows were kept dust and oil free with detergent and soft tissue. A 12-bit analogue-to-digital convertor was incorporated in the interface electronics to provide a 0.02% resolution.

The counter developed here operated on a light blockage principle theoretically covering the range 10–465 μm, but in practice 10–200 μm (see below). A relatively large volume of water was sampled for one counting cycle (150 ml per 16-s cycle) which allowed statistically good samples within the size range quoted. Water was pumped through a 600 μm × 2.5 mm cell across which a collimated (600 μm diameter) light beam was passed to a photodetector. The output of the detector was amplified, integrated and used to provide a feedback voltage to the lamp drive circuit, producing a steady state reference voltage irrespective of lamp ageing and, within limits, water turbidity. Any particle moving through the beam produced a voltage drop in the photodetector, the

amplitude of which was proportional to the particle area. The precalibrated comparators received the signal, the outputs of which were connected to 16-bit counters.

Calibration in the laboratory used latex bead standards of known mean diameter. The comparator settings for each of the 16 channels were read from the calibration curve of voltage vs diameter. The data were presented as cumulative number distributions; the cut-offs for each channel are given in Table 2.

Also, a facility to monitor the 1-s record of the first channel, i.e. all particles >10 μm, was included for work at sea in order to identify small scale features and "spikes"; the latter were thought to be due to the fragmentation of large particles. To prevent large particles (>2 mm) entering the cell, a mesh was placed over the inlet funnel.

A second G9M4 motor and Austin pump provided the flow and this motor was powered by a separate battery pack similar to those described above, except that the cells were connected in 16 V blocks in order to give the optimum flow of 600 ml min^{-1} for 8 h. Flow was monitored by using the cell as a Venturi and coupling a modified Appleby and Ireland differential pressure transducer across it.

Table 2. Channel number and the equivalent diameter cut-off for the cumulative number distribution ($N_{>d}$ – a d). The geometric means are used for difference distribution calculations

Channel (no.)	Diameter (μm)	Geometric mean ($\bar{d}$)
CHAN 1	10.0	
		11.4
CHAN 2	12.9	
		14.7
CHAN 3	16.7	
		19.0
CHAN 4	21.6	
		24.5
CHAN 5	27.9	
		31.6
CHAN 6	36.0	
		40.9
CHAN 7	46.4	
		52.8
CHAN 8	59.9	
		68.2
CHAN 9	77.4	
		88.0
CHAN 10	100.0	
		114.0
CHAN 11	129.2	
		147.0
CHAN 12	166.9	
		190.0
CHAN 13	215.9	
		245.0
CHAN 14	287.5	
		316.0
CHAN 15	359.5	
		409.0
CHAN 16	464.5	

Height off-bottom. A near-bottom echo sounder was fitted for working close to the sea floor, i.e. <10 m. It consisted of a 35 kHz transponder facing downward. The transmission pulse was used to gate an 8-bit binary counter which was stopped by the reflected pulse. The counter clock pulses were chosen to give a resolution of 1 m and a maximum depth indication of 256 m off the bottom. The binary data were then inserted into the data stream for decoding and displaying on the deck monitor. Due to the width of the transmission pulse and local ranging, the minimum depth that could be observed was approximately 9 m off-bottom. For working closer to the sea floor, a weight was suspended beneath the rig connected to a no-load alarm.

Data transmission. All the output signals from the sensors were reduced to a common format of binary-coded 8-bit words after the necessary interfacing. Depending on the resolution required, one or two 8-bit words were coupled to the sensors. The data words were loaded to parallel input-serial output interconnected registers from which the data were serially shifted at 2 Hz rate into the transmission line drive circuitry. During the 16-s cycle of the particle counter, the data from the counters were fed to a multiplexor, thus the data from each sample cycle were transmitted twice. Comparison of the repeated cycle was used to look for electronic noise in the data. Sub-multiplexing was also found to be advantageous for transmitting data of the instrument functions, e.g. battery volts, flow through the filters. Prior to transmission, a start bit and two stop bits were added to each 8-bit word to produce 11-bit words. The signal was then modulated with $3\frac{1}{3}$ and $6\frac{2}{3}$ kHz representing "0" and "1" levels, respectively, thus providing a frequency shift keying (FSK) signal suitable for transmission via a single core conducting cable to the shipboard equipment.

Data handling at sea and in the laboratory

As mentioned above, the main reason for real-time, i.e. within seconds from sensing via calibration and editing to display, was to carry out informed sampling on the return cast. The data were edited to reject bad data and particle counts fitted to linear log-log distributions to aid comprehension. In the laboratory the data were averaged over depth intervals on a number of data cycles depending on the purpose of the analysis.

Ship. The data from the instrument passed to a Neil-Brown CTD deck unit or to an IOS FSK demodulator. These units demodulated the FSK line signal and converted the binary data into binary-coded decimal (bcd) format. During the course of a station, the data from the instrument also were recorded directly on to a REVOX analogue tape recorder for back-up purposes, and the IOS demodulator allowed double-speed replays of these tapes if any calibrations were to be altered.

Data were displayed on the CTD deck unit and a second purpose-built unit. A BBC micro-computer acted as full instrument monitor. Output from the deck units could also be fed to analogue chart recorders, printers and the main ship's computer. The computer system on R.R.S. *Discovery* was described by LEWIS and JACKSON (1983). The sampling program was purely data-driven so that it would cope with frames arriving both at the "normal" on-station data rate of two frames per second, and also the double-speed REVOX playbacks, without any modification.

The arrival of raw data on disc activated the processing software (LUNN and LEWIS, unpublished data) which demultiplexed and calibrated the data, channel by channel, and wrote it on a separate disc file. The arrival of calibrated data in turn activated the display and secondary processing programmes (linear regression, particle mass concentration,

Table 3. Averaged data for Sta. 10554. Averages are for nine "good" particle cell cycles (see text). Values in parentheses are standard errors. Particle data is expressed as $\log N_{>10} = \log a - m \log d$ *for particles between 10 and 174 μm*

Average depth z (m)	Intercept $\log a$ (no. $l^{-1} > 10$)	Gradient m (no. l^{-1} μm^{-1})	Correlation coefficient r	Volume V (ppb)	Attenuation c (m^{-1})	Temperature T (°C)	Salinity S (‰)
41	4.006	−2.615	0.995	66.5	0.4533	20.89	36.835
(15)	(0.152)	(0.082)		(13.0)	(0.0073)	(0.82)	(0.070)
123	3.863	−2.414	0.997	69.1	0.4292	18.72	36.785
(25)	(0.112)	(0.061)		(11.8)	(0.0125)	(0.22)	(0.092)
207	3.706	−2.345	0.996	52.1	0.4050	18.00	36.606
(37)	(0.126)	(0.068)		(10.8)	(0.0043)	(0.78)	(0.225)
348	3.548	−2.504	0.997	29.1	0.3978	14.90	36.0533
(35)	(0.121)	(0.065)		(7.1)	(0.0020)	(0.65)	(0.191)
474	3.411	−2.526	0.995	15.8	0.3921	13.07	35.797
(62)	(0.144)	(0.078)		(7.0)	(0.0019)	(0.69)	(0.169)
685	3.210	−2.397	0.996	15.2	0.3872	11.34	35.611
(57)	(0.129)	(0.070)		(43.3)	(0.008)	(0.37)	(0.140)
883	3.314	−2.766	0.989	11.7	0.3850	9.79	35.557
(53)	(0.244)	(0.136)		(1.3)	(0.004)	(0.47)	(0.125)
1063	3.203	−2.500	0.995	10.3	0.3838	8.59	35.581
(52)	(0.152)	(0.082)		(4.1)	(0.005)	(0.33)	(0.118)
1297	3.048	−2.009	0.997	15.4	0.3826	7.56	35.549
(98)	(0.093)	(0.005)		(7.4)	(0.004)	(0.48)	(0.128)
1515	3.122	−2.401	0.997	9.8	0.3820	6.36	35.389
(52)	(0.107)	(0.058)		(4.2)	(0.001)	(0.31)	(0.125)
1695	3.044	−2.255	0.997	14.1	0.3813	5.46	35.289
(54)	(0.103)	(0.056)		(4.0)	(0.0003)	(0.22)	(0.121)
1931	3.050	−2.560	0.995	8.1	0.3806	4.61	35.177
(69)	(0.148)	(0.083)		(2.8)	(0.0002)	(0.21)	(0.121)
2141	3.023	−2.485	0.993	8.7	0.3801	4.01	35.089
(58)	(0.174)	(0.094)		(3.1)	(0.0002)	(0.13)	(0.117)
2376	3.088	−2.749	0.997	6.9	0.3801	3.55	35.033

(70)	(0.125)	(0.070)		(1.5)	(0.0001)	(0.12)	(0.115)
2634	3.003	-2.458	0.993	10.5	0.3803	3.19	34.989
(96)	(0.169)	(0.091)		(3.2)	(0.0001)	(0.11)	(0.113)
2936	3.016	-2.610	0.988	6.0	0.3803	2.89	34.957
(82)	(0.253)	(0.145)		(0.9)	(0.0001)	(0.06)	(0.112)
3139	3.012	-2.398	0.991	11.7	0.3801	2.75	34.943
(12)	(0.190)	(0.103)		(3.2)	(0.0001)	(0.01)	(0.111)
3134	2.898	-2.257	0.994	8.7	0.3802	2.73	34.942
(19)	(0.152)	(0.085)		(2.2)	(0.0001)	(0.01)	(0.111)
3360	3.024	-2.851	0.984	5.6	0.3805	2.65	34.931
(77)	(0.304)	(0.169)		(1.3)	(0.0001)	(0.03)	(0.111)
3614	2.957	-2.345	0.996	7.4	0.3806	2.57	34.918
(72)	(0.123)	(0.067)		(4.4)	(0.0001)	(0.02)	(0.111)
3934	2.888	-2.477	0.992	9.6	0.3806	2.51	34.906
(161)	(0.181)	(0.098)		(3.4)	(0.0000)	(0.03)	(0.111)
4347	2.924	-2.456	0.993	8.7	0.3807	2.46	34.894
(72)	(0.175)	(0.095)		(2.8)	(0.0001)	(0.01)	(0.111)
4610	2.841	-2.088	0.997	11.0	0.3810	2.44	34.888
(69)	(0.097)	(0.053)		(4.5)	(0.0001)	(0.00)	(0.111)
4836	2.890	-2.262	0.996	8.5	0.3814	2.45	34.884
(54)	(0.117)	(0.065)		(1.7)	(0.0001)	(0.00)	(0.111)
5053	2.940	-2.087	0.998	16.9	0.3824	2.46	34.882
(87)	(0.080)	(0.043)		(4.0)	(0.0005)	(0.01)	(0.111)
5335	3.068	-2.536	0.994	8.9	0.3841	2.49	34.879
(67)	(0.169)	(0.094)		(2.8)	(0.0005)	(0.01)	(0.111)
5422	3.128	-2.551	0.995	9.4	0.3844	2.50	34.879
(2.2)	(0.144)	(0.078)		(4.1)	(0.0001)	(0.00)	(0.111)
5432	3.198	-2.21	0.989	22.2	0.3846	2.50	34.878
(2.5)	(0.190)	(0.103)		(5.5)	(0.0003)	(0.00)	(0.111)
5434	3.029	-2.003	0.998	15.0	0.3844	2.50	34.878
(0.88)	(0.078)	(0.043)		(9.2)	(0.0000)	(0.00)	(0.111)
5434	3.090	-2.249	0.994	18.0	0.3845	2.50	34.878
(0.2)	(0.149)	(0.081)		(4.6)	(0.0001)	(0.00)	(0.111)

particle mass flux, etc.). Real-time records (e.g. Fig. 6) of any four dependent variables against any chosen independent variable could be plotted. The data required some editing; there were some interruptions in the data stream and some spikes in the record, e.g. at 67 min.

The merging with CTD data, editing and averaging of data were conducted in the laboratory, and were controlled primarily by the "good" particle counter data. The synchronization of data was checked and the correlation coefficient of the regression line of log cumulative number concentrations vs log diameter of the particles was calculated. Before a distribution was passed as "good", a correlation coefficient of ≥ 0.97 was required (BRUN-COTTAN, 1976). Mean and standard errors of cumulative number distributions and CTD data were calculated using a specified number of good cycles. It was found that a high standard error resulted from the low probability of sampling particles >200 μm; essentially this made the last four channels redundant. Thus the results in Table 3 are given for the first 12 channels or 10–174 μm particles; nine successive cycles were taken for averaging giving a reasonable compromise between reducing the noise in the higher channels and yet maintaining spatial resolution. The regressions, volumes, masses, fluxes and their standard errors were calculated from that averaged distribution. Of 375 cycles on the outward cast shown in Fig. 6, 270 met the editing criteria of good distributions. Rejected data could be inspected in the original listings.

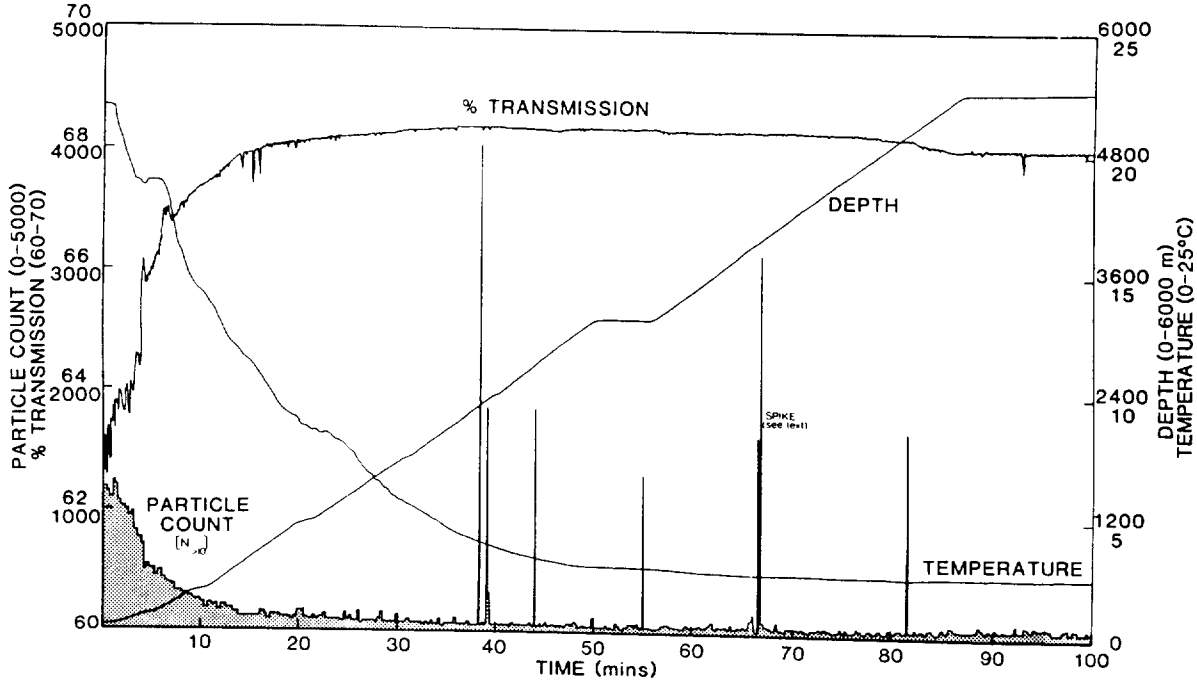

Fig. 6. Ship's record of temperature, depth, percent transmission and particle counts (all particles >10 μm, not flow corrected) against time.

DISCUSSION

Validation of particle data

The measured transmission (Tr) was expressed as attenuation coefficient, c ($Tr = e^{-cl}$, where l is the path length in metres). The linear regression equation of c against all particles >10 μm ($N_{>10}$) was given by

$$c = 8.46 \times 10^{-6} N_{>10} + 0.375 \qquad r = 0.996 \qquad n = 30.$$

The correlation was good, i.e. the two instruments were sensing the same populations.

The particle cumulative number distributions in the size range studied here by optimal counting were contiguous with those given by LAMBERT *et al.* (1981; scanning electron microscopy, 0.1–10 μm), MCCAVE (1975; impedance counting, 1–32 μm) and HONJO *et al.* (1984; >200 μm, camera system) (Fig. 7). The distribution was consistent with a log-normal form, yet the often used approximations to straight line fits ($\log N_{>d} = \log a - m \log d$, where $d \geq 1$) hold between narrow ranges.

A further rough check that the size distributions and changes in gradient (m) are consistent is to compare the volume concentration of particles (ppb) with the attenuation coefficient. The volume of particles between sizes d_1 and d_2 is given by

$$V = \frac{-a\,\pi m}{6(m-3)} [d^{m-3}]_{d_1}^{d_2} \text{ for } m \neq 3 \text{ (MCCAVE, 1975).}$$

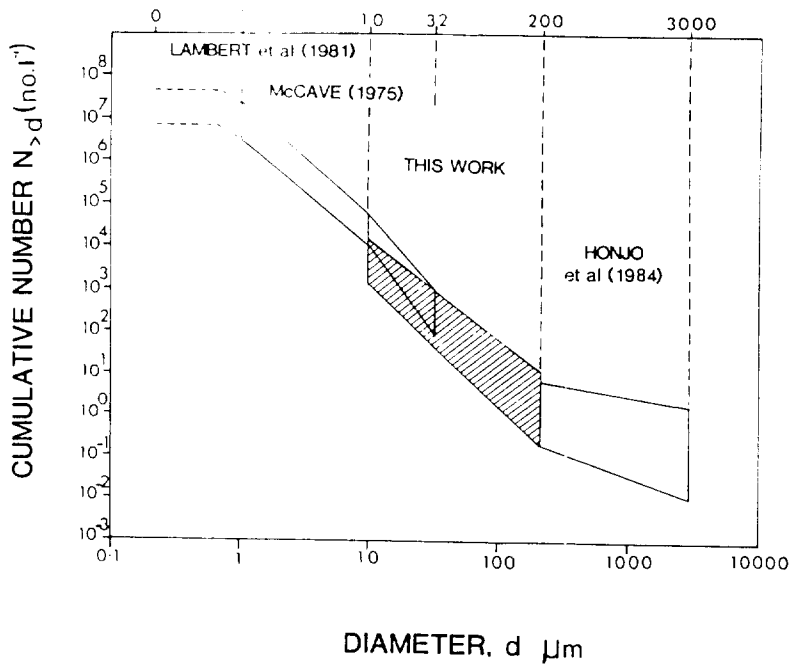

Fig. 7. Particle concentration against particle diameter spectrum expressed as $\log N_{>d}$ vs $\log d$. The top line represents surface waters and the bottom mid-waters. The range of operation for each study is given by the dashed vertical lines.

Table 4. Data summary for Sta. 10554

Average depth z (m)	Intercept log a (no. $l^{-1} > 10$)	Gradient m (no. l^{-1} μm $^{-1}$)	Correlation coefficient r	Volume V_m (ppb)	Attenuation c (m^{-1})	Temperature T (°C)	Salinity S (‰)
Summary:							
Surface (n = 54)							
313	3.703	−2.477	0.997	41.3	0.4108	16.15	36.281
(223)	(0.114)	(0.062)		(4.7)	(0.0241)	(3.39)	(0.496)
Midwater (n = 171)							
2870	3.033	−2.429	0.997	9.9	0.3812	4.16	35.095
(1270)	(0.110)	(0.060)		(0.9)	(0.00014)	(2.26)	(0.251)
Deep water (n = 47)							
5412	3.095	−2.252	0.997	15.1	0.3844	2.50	34.879
(48)	(0.104)	(0.056)		(2.7)	(0.0003)	(0.01)	(0.074)

Taking a value of log $a = 6.5$ ($a = 3.5 \times 10^6$) at 1 μm and a gradient, m, of 2.7 (McCave, 1975), the volume between 1.26 and 32 μm (McCave, 1983), V_s, is 29 ppb. For the medium-sized particles (10–174 μm) the mean gradient was 2.4 (Table 4) hence the equivalent 1 μm intercept value will be

$$\log a = (6.5 - 2.7 + 2.4) = 6.2 \qquad (a = 1.6 \times 10^6)$$

assuming that the 10 μm values of log N are the same. The resulting volume, V_m, is 61 ppb and the ratio $V_m{:}V_s = 2.1$.

McCave (1983) gave the relationship of attenuation coefficient to volume concentration of 1.26–32 μm particles as determined by Coulter Counter which, in practice, measures particle volume to be

$$c = 2.016 \times 10^{-3} V_s + 0.410,\ n = 186,\ r = 0.93.$$

The volumes in Table 3 were calculated from the particle counter data, assuming equivalent sphere diameters of a technique which effectively measures area. Taking the geometric means between d_i and $d_{i+1} = \bar{d}_i$ the total volume concentration for the first 12 channels, V_m, is $\Sigma n_i \pi \bar{d}_i^3/6$. From Table 3 the linear regression equation of attenuation coefficient against V_m is given by

$$c = 9.088 \times 10^{-4} V_m + 0.372,\ n = 30,\ n = 0.93.$$

The ratio of $V_m{:}V_s = 2.2$ from the above two equations, close to that calculated from the distribution example. Therefore, the volume estimates appear consistent. However, the constants in the two equations are different (0.41 and 0.37); for clean seawater at 660 nm, c should equal 0.41. The 10% error in our zero value is due to calibration error. Essentially, the convergence of the three checks gives us confidence in the particle counter measurements.

Validation of sampling efficiency

The elemental concentrations for 1–60 μm particles, collected in 1 μm porosity membranes after prefiltration through a 60 μm mesh, were determined by instrumental neutron activation analysis performed at the Laboratoire "Pierre-Süe" at Saclay, France [see Buat-Menard *et al.* (1980) for methodology]. The results are presented in Table 5. The concentrations are somewhat lower than those determined for the GEOSECS and MIDATLANTE-MADCAP campaigns (Buat-Menard, 1979) but this is probably due to the use of 1 μm porosity membranes in this work against 0.4 μm membranes in earlier work. The consistency is best appreciated by comparing the crustal enrichment factors (Table 5b) with those presented in Buat-Menard (1979) and Buat-Menard and Chesselet (1979) for Atlantic intermediate and deep waters (Fig. 8). The enrichments are similar and there is no evidence of contamination (even for Fe).

The small particle scanning electron microscope energy dispersive X-ray data (Fig. 9) reflect the Sc (clays)-Ca (coccoliths) changes with depth (Table 5a). The abundance of the calcite in surface samples precluded the identification of clays in this sample but, as can be seen, the clay component became more evident with depth. The high Sc concentrations and clay abundance in deep waters (Table 5a, Fig. 9) reflect the resuspension-horizontal transport processes as indicated by the particle profiles (Fig. 6 and Table 3).

Table 5a. Particulate element concentration (ng l^{-1}), 1–60 μm *particles*

	134 m	1320 m	1806 m	5470 m
Sc	0.0034	0.0105	0.0105	0.0295
Th	0.0038	0.0116	0.0118	0.028
Fe	13.45	36.38	54.22	87.3
Co	0.0307	0.0505	0.0799	0.0759
Sb	0.0279	0.0528	0.0834	0.0245
Ag	0.0103	0.2537?	0.0350	0.0134
Se	0.0711	0.0516	0.0507	0.0279
Hg	0.1040	0.0513	0.1307	0.0721
Au	0.0042	0.0428?	0.0060	0.0032
Ca	1242	812	503	475

Table 5b. Crustal enrichment factors:

$E.F._{x} = ([Element]/[Sc])_{particles}/([Element]/[Sc])_{crust}$

	134 m	1320 m	1806 m	5470 m	$([El]/[Sc])_{crust}$
Th	2.6	2.5	2.7	2.2	0.436
Fe	1.5	1.4	2.0	1.2	2559
Co	7.9	4.2	6.7	2.3	1.136
Sb	903	553	873	91	9.091×10^{-3}
Ag	953		1048	143	3.182×10^{-3}
Se	9212	5.3	2130	417	2.272×10^{-3}
Hg	8400	4.7	3419	671	3.636×10^{-3}
Au	6790		3140	60	1.818×10^{-4}

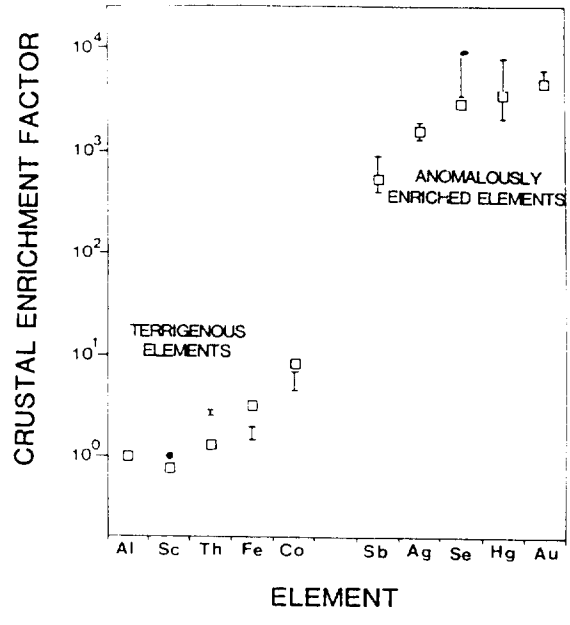

Fig. 8. Comparison of crustal enrichment factors for some elements. □ BUAT-MENARD and CHESSELET (1979) (taking Al as unity). I This work (taking Sc as unity).

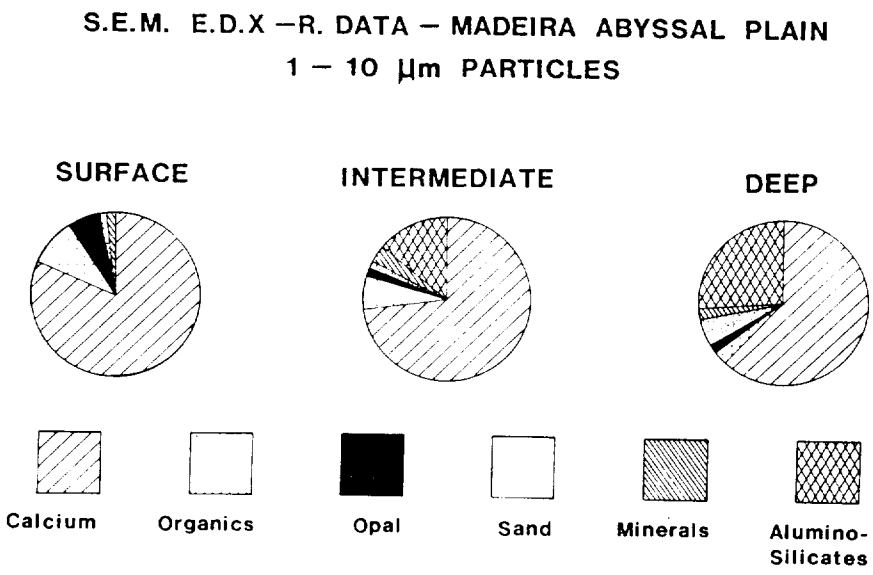

Fig. 9. Scanning electron microscope—energy dispersive X-ray analysis of small particles showing relative abundance of major forms.

CONCLUSIONS

The instrument meets the requirements of sampling suspended particles in the deep ocean. Samples can be taken in an informed manner and free from contamination. The data from the new particle counter reported in the literature fill in the "missing" information between small and large particles. Results from the particle counter will be used to model particle mass and flux distributions with a view to looking at the processes of recycling, dissolution, resuspension and transport. The data from chemical analysis of particles and water can be fed into these models.

Acknowledgements—The authors are indebted to colleagues at IOS in the engineering and computing groups. Thanks are due to David Northey and John Hollyhead of Northey International Systems Ltd for loan of equipment and assistance in calibration of the particle counter, to Nicholas Risler of the CNRS, Gif-sur-Yvette, who performed the INAA at the Laboratoire "Pierre-Süe" at Saclay, France, to Gill Gibbs of the Microstructural Sciences Unit, University of Surrey, for the S.E.M. work, and to Claude Lambert (CNRS) for comments on the script and general encouragement. We also extend our gratitude to the officers and crew of R.R.S. *Discovery*.

This research has been carried out under contract for the Department of the Environment as part of its radioactive waste management research programme. The results will be used in the formulation of Government policy but, at this stage, do not necessarily represent Government policy.

REFERENCES

BACON M. P. and R. F. ANDERSON (1982) Distribution of thorium isotopes between dissolved and particulate forms in the deep sea. *Journal of Geophysical Research*, **87**, 2045–2056.

BARTZ R., J. R. V. ZANEVELD and H. PAK (1978) A transmissometer for profiling and moored observations in water. *Proceedings of the Society of Photo-optical Instrumentation Engineers*, **160** (Ocean Optics V), 102–108.

BEER R. M., J. P. DAUPHIN and T. S. SHOLES (1974) A deep-sea, *in situ*, suspended sediment sampling system. *Marine Geology*, **17**, M35–M44.

BISHOP J. K. B. and J. M. EDMOND (1976) A new large volume filtration system for the sampling of oceanic particulate matter. *Journal of Marine Research*, **34**, 181–198.

BISHOP J. K. B., R. W. COLLIER, D. R. KETTEN and J. M. EDMOND (1980) The chemistry, biology and vertical flux of particulate matter from the upper 1500 m of the Panama Basin. *Deep-Sea Research*, **27**, 615–640.

BOYD C. M. and G. W. JOHNSON (1969) Studying zooplankton populations with an electronic zooplankton counting device and LINC-B computers. In: *Transactions of the Applications of Sea-Going Computers Symposium*, J. D. MUDIE and C. B. JACKSON, editors, Marine Technology Society, Washington D.C., pp. 83–90.

BROWN J. C. (1977) A microprocessor-based oceanographic particle data collection system. Oceans 1977 Conference Record. Marine Technology Society, Washington D.C., 3C, pp. 1–4.

BRUN-COTTON J.-C. (1976) Stokes settling and dissolution rate model for marine particles as a function of size distribution. *Journal of Geophysical Research*, **81**, 1601–1606.

BUAT-MENARD P. (1979) Influence de la retombée atmospherique sur la chimie des metaux en trace dans la matiere en suspension de l'Atlantique Nord. D.Sc. Thesis, Université de Paris VII, 434 pp.

BUAT-MENARD P. and R. CHESSELET (1979) Variable influence of the atmospheric flux on the trace metal chemistry of oceanic suspended matter. *Earth and Planetary Science Letters*, **42**, 399–411.

BUAT-MENARD P., C. E. LAMBERT, M. ARNOLD and R. CHESSELET (1980) Multi-element neutron activation analysis measurements towards the geochemistry of particulate matter exchange between continent–atmosphere–ocean. *Journal of Radioanalytical Chemistry*, **55**, 445–452.

HONJO S., K. W. DOHERTY, Y. C. AGRAWAL and V. L. ASPER (1984) Direct optical assessment of large amorphous aggregates (marine snow) in the deep ocean. *Deep-Sea Research*, **31**, 67–76.

KRISHNASWAMI S., D. LAL, B. L. M. SOMAYAJULU, R. F. WEISS and H. CRAIG (1976) Large-volume *in situ* filtration of deep Pacific waters: mineralogical and radioisotope studies. *Earth and Planetary Science Letters*, **32**, 420–429.

LAIRD J. C., D. P. JONES and C. S. YENTSCH (1967) A submersible batch filtering unit. *Deep-Sea Research*, **14**, 251–252.

LAMBERT C. E., C. JEHANNO, N. SILVERBERG, J.-C. BRUN-COTTON and R. CHESSELET (1981) Log-normal distributions of suspended particles in the open ocean. *Journal of Marine Research*, **39**, 77–98.

LERMAN A. (1979) *Geochemical processes—water and sediment environments*. Wiley, New York, 481 pp.

LEWIS A. R. and C. S. JACKSON (1983) Changing from single to multi-processor systems for real-time computing in oceanographic research. *Proceedings of the Digital Equipment Computer Users Society*, Zurich, pp. 393–397.

MADDUX W. S. and J. W. KANWISHER (1965) An *in situ* particle counter. *Limnology and Oceanography* (Supplement), R162–168.

MCCAVE I. N. (1975) Vertical flux of particles in the ocean. *Deep-Sea Research*, **22**, 491–502.

MCCAVE I. N. (1983) Particulate size spectra. Behaviour and origin of nepheloid layers over the Nova Scotian Continental Rise. *Journal of Geophysical Research*, **88**, 7647–7666.

MCCAVE I. N. (1984) Size spectra and aggregation of suspended particles in the deep ocean. *Deep-Sea Research*, **31**, 329–352.

SIMPSON W. R. (1982) Particulate matter in the oceans—sampling methods, concentration, size distribution and particle dynamics. *Oceanography and Marine Biology Annual Review*, **20**, 119–172.

SPENCER D. W. and P. L. SACHS (1970) Some aspects of the distribution, chemistry and mineralogy of suspended matter in the Gulf of Maine. *Marine Geology*, **9**, 117–136.

DOCUMENT DATA SHEET

AUTHOR	SIMPSON, W.R.	*PUBLICATION DATE* 1987
TITLE	Suspended particulate studies over the Madeira Abyssal Plain.	
REFERENCE	Institute of Oceanographic Sciences Deacon Laboratory, Report, No. 252, 86pp.	

ABSTRACT

Various aspects relating to suspended particulate matter over the Madeira Abyssal Plain are discussed including size distributions, morphology, chemistry, microbiology, particle mass concentration and particle fluxes. The period covered in the report is 1982 to 1987.

A deep water particle sampler and sensor package developed within this contract is fully described, as is the validation of the results obtained from it. Comparisons are made with long-term transmissometer/current meter moorings and sediment trap moorings.

The main conclusions are that (i) the nepheloid layer over the Madeira Abyssal Plain is weak (5 mg m^{-3} over background concentration) supported by current meter data; (ii) the nepheloid layer is transported to the site; (iii) the only particles likely to be moved from the site are small (1-2 μm) organic particles; (iv) bacteria are likely to form the bulk of these particles and have a surface area available to adsorp metals many tens of times greater than the minerals present; (v) the fluxes at GME are low (25 mg m^{-2} d^{-1}); (vi) 40% of that flux is remineralised; (vii) by analogy to the REE, based on data and theory, Th and Pu may behave like Ce, Ac like La, and Am like the light REE; (viii) radionuclides released into the water and adsorped on to bacteria may travel great distances until either particle loading or biological activity remove them from the system.

ISSUING ORGANISATION	Institute of Oceanographic Sciences Deacon Laboratory Wormley, Godalming Surrey GU8 5UB. UK. Director: Dr A S Laughton FRS	*TELEPHONE* 0428 79 4141 *TELEX* 858833 OCEANS G *TELEFAX* 0428 79 3066

KEYWORDS	*NEPHELOID LAYER* *PARTICLE CONCENTRATION* *PARTICLE COUNTER* *PARTICULATE FLUX* *SEDIMENT TRAPS* *SUSPENDED MATTER* *TRANSMISSOMETER* *MADEIRA ABYSSAL PLAIN*	*CONTRACT* PECD 7/9/214 *PROJECT* CO 33 *PRICE*